

Extreme value statistics of correlated random variables: a pedagogical review

Satya N. Majumdar,¹ Arnab Pal,² and Grégory Schehr¹

¹*LPTMS, CNRS, Univ. Paris-Sud, Université Paris-Saclay, 91405 Orsay, France*

²*School of Chemistry, The Center for Physics and Chemistry of Living Systems,*

The Raymond and Beverly Sackler Center for Computational Molecular and Materials Science,

& The Mark Ratner Institute for Single Molecule Chemistry, Tel Aviv University, Tel Aviv 6997801, Israel

060

Abstract
in arXiv:1806.05465
published in
Journal of Statistical Mechanics
2018
https://doi.org/10.1088/1751-8752/aab111
arXiv:1806.05465v1 [cond-mat.str-el] 20 Jun 2018

CONTENTS

I. Introduction	2
II. Extreme value statistics: basic preliminaries	3
III. Independent and Identically distributed random variables	4
A. Parent distributions with a power law tail	4
B. Parent distributions with a faster than power law tail	4
1. The exponential case $p(x) = e^{-x}$ for $x \geq 0$	5
2. The Gaussian case $p(x) = \frac{1}{\sqrt{2\pi}}e^{-x^2/2}$	5
C. Parent distributions with an upper bounded support	6
D. Order statistics	6
IV. Correlated random variables	7
A. Weakly correlated random variables	7
B. Strongly correlated random variables	8
1. One-dimensional Brownian motion and random walks	9
2. Ornstein-Uhlenbeck (OU) process	11
3. Extreme statistics in the presence of a global constraint	12
4. Hierarchically and logarithmically correlated random variables	14
5. Extreme statistics in stochastic resetting systems	16
6. Extreme statistics for fluctuating interfaces in one-dimension: an example of a strongly correlated random variable	18
7. Extreme statistics in random matrix theory	20
8. Extreme statistics of trapped fermions	23
C. Other extreme value problems	24
1. Density of near-extremes	24
2. The time at which the maximum/minimum is reached	25
3. Records	26
V. Summary and Conclusion	27
Acknowledgments	27
A. Some details about the Tracy-Widom distribution	28
B. From noninteracting fermions in a harmonic trap at $T = 0$ to random matrices	29
References	30

I. INTRODUCTION

Extreme events are ubiquitous in nature. They may be rare events but when they occur, they may have devastating consequences and hence are rather important from practical points of view. To name a few, different forms of natural calamities such as earthquakes, tsunamis, extreme floods, large wildfire, the hottest and the coldest days, stock market risks or large insurance losses in finance, new records in major sports events like Olympics are typical examples of extreme events. There has been a major interest to study these events systematically using statistical methods and the field is known as Extreme Value Statistics (EVS) [1–4]. This is a branch of statistics dealing with the extreme deviations from the mean/median of probability distributions. The general theory sets out to assess the type of probability distributions generated by processes which are responsible for these kinds of highly unusual events. In recent years, it has been realized that extreme statistics and rare events play an equally important role in various physical, biological and financial contexts as well—for a few illustrative examples (by far not exhaustive) see [5–71]. A typical example can be found in disordered systems where the ground state energy, being the minimum energy, plays the role of an extreme variable. In addition, the dynamics at low temperatures in disordered systems are governed by the statistics of the highest energy barrier in the system. Hence the study of extremes and related quantities is extremely important in the field of disordered systems [5–7, 10, 12, 14, 19, 50, 71–75]. A rather important physical

system where extreme fluctuations play an important role corresponds to fluctuating interfaces in the Edwards-Wilkinson or Kardar-Parisi-Zhang universality classes [16, 18, 23, 24, 27, 35, 76, 77]. Another exciting recent area concerns the distribution of the largest eigenvalue in random matrices: the limiting distribution [8, 9] and the large deviation probabilities [78–80] of the largest eigenvalue and its various applications (for a recent review on the largest eigenvalue of a random matrix, see [81]). Extreme value statistics also appears in computer science problems such as in binary search trees and related search algorithms [11, 12, 17, 20, 22].

In the classical extreme value theory, one is concerned with the statistics of the maximum (or minimum) of a set of *uncorrelated* random variables (see e.g. the classical textbooks [2, 4] or the review [66]). In contrast, in most of the physical systems mentioned above, the underlying random variables are typically *correlated*. In recent years, there have been some advances in the understanding of EVS of correlated variables. In this survey, we will first review the classical EVS of uncorrelated variables. Then we will discuss the EVS of *weakly* correlated random variables with some examples. Finally few examples of *strongly* correlated random variables will be discussed.

This subject of EVS is rapidly evolving and this is a short review on some of the recent developments and the key-questions in the field. The purpose of this review is not to provide detailed calculations for different models, but rather point out to the reader the relevant questions, recent developments and the relevant references. The interested reader can look up this literature for details. The choice of topics reflects our personal taste and contributions to the field and, by no means, is exhaustive. Hence, the list of references is clearly far from being exhaustive and any inadvertent omission of a relevant reference is apologized.

II. EXTREME VALUE STATISTICS: BASIC PRELIMINARIES

In a given physical situation, one needs to first identify the set of relevant random variables $\{x_1, x_2, \dots, x_N\}$. For example, for fluctuating one-dimensional interfaces, the relevant random variables may denote the heights of the interface at different space points. In disordered systems such as spin glasses, $\{x_i\}$'s may denote the energy of different spin configurations for a given sample of quenched disorder. Once the random variables are identified, there are subsequently two basic steps involved : (i) to compute explicitly the joint distribution $P(\{x_i\})$ of the relevant random variables (this is sometimes very difficult to achieve) and (ii) from the joint distribution $P(\{x_i\})$ calculate the distribution of some observables, such as the sample mean or the sample maximum, defined as

$$\text{mean } \bar{X} = \frac{x_1 + x_2 + \dots + x_N}{N}, \quad (1)$$

$$\text{maximum } M = \max(x_1, x_2, \dots, x_N). \quad (2)$$

Particular simplifications occur for independent and identically distributed (IID) random variables, where the joint distribution $P(\{x_i\})$ factorizes, i.e., $P(x_1, x_2, \dots, x_N) = p(x_1)p(x_2)\dots p(x_N)$, where each variable is chosen from the same parent probability density $p(x)$. Knowing the parent distribution $p(x)$, one can then easily compute the distributions, e.g., of \bar{X} and of M .

For example, let us first consider \bar{X} . One knows that irrespective of the choice of the parent distribution (with finite variance) the probability distribution function (PDF) of the *mean* of N IID random variables tends to a Gaussian distribution for large N namely,

$$P(\bar{X}, N) \xrightarrow{N \rightarrow \infty} \frac{1}{\sqrt{2\pi\sigma^2/N}} e^{-\frac{N}{2\sigma^2}(\bar{X}-\mu)^2}, \quad (3)$$

where μ and σ^2 are the mean and the variance of the parent distribution respectively. This is known as the *Central Limit Theorem* [133] and this Gaussian form is universal. However, for correlated variables, one does not know, in general, how to compute the distribution of \bar{X} and a priori one expects that the limiting distribution of \bar{X} will be different from a Gaussian (see for instance [26] for a discussion of this question in connection with extreme statistics).

Similar question about universality also arises for the distribution of extremes, e.g., that of M in Eq. (2). We will see below that, as in the case of the mean \bar{X} , there exist universal limit laws for the distribution of the maximum M for the case of IID variables. However, for *strongly* correlated variables, the issue of universality is wide open. Suppose that we know the joint distribution $P(\{x_i\})$ explicitly. Then to compute the distribution of the maximum M , it is useful to define the cumulative distribution of M which can be easily expressed in terms of the joint distribution

$$Q_N(x) = \text{Prob}[M \leq x, N] = \text{Prob}[x_1 \leq x, x_2 \leq x, \dots, x_N \leq x], \quad (4)$$

$$= \int_{-\infty}^x dx_1 \int_{-\infty}^x dx_2 \cdots \int_{-\infty}^x dx_N P(x_1, x_2, \dots, x_N), \quad (5)$$

and the PDF of the maximum can be obtained by taking the derivative i.e. $P(M, N) = Q'_N(M) \equiv \frac{dQ_N}{dx}|_{x=M}$.

III. INDEPENDENT AND IDENTICALLY DISTRIBUTED RANDOM VARIABLES

For IID random variables, the joint PDF factorizes and we get

$$Q_N(x) = \left[\int_{-\infty}^x dy p(y) \right]^N = \left[1 - \int_x^{\infty} dy p(y) \right]^N. \quad (6)$$

This is an exact formula for the cumulative distribution of the maximum for any N . Evidently, $Q_N(x)$ depends explicitly on the parent distribution $p(x)$ for any finite N . The question is: as in the CLT of the sum of random variables discussed before, does any universality emerge for $Q_N(x)$ in the large N limit? The answer is that indeed a form of universality emerges in the large N limit, as we summarize below.

It turns out that in the scaling limit when N is large, x is large, with a particular scaling combination (see below) fixed, $Q_N(x)$ approaches a limiting form:

$$Q_N(x) \xrightarrow[z=(x-a_N)/b_N \text{ fixed}]{x \rightarrow \infty, N \rightarrow \infty} F\left(\frac{x-a_N}{b_N}\right) \quad (7)$$

equivalently, $\lim_{N \rightarrow \infty} Q_N(a_N + b_N z) = F(z)$ (8)

where a_N , b_N are non-universal scaling factors that depend on the parent distribution $p(x)$, but the scaling function $F(z)$ can only be of the three possible forms $F_{1,2,3}(z)$ depending only on the large x tail of the parent distribution $p(x)$. This is known as the Gnedenko's classical law of extremes [3].

A. Parent distributions with a power law tail

We consider the IID random variables whose parent distribution has a power law convergence $p(x) \sim Ax^{-(1+\alpha)}$ with $A, \alpha > 0$. In this case, we denote the scaling function as $F_1(z)$ and this is found to be

$$F_1(z) = \begin{cases} e^{-z^{-\alpha}} & \text{for } z \geq 0 \\ 0 & \text{for } z \leq 0. \end{cases} \quad (9)$$

The PDF is given by

$$f_1(z) = F_1'(z) = \frac{\alpha}{z^{\alpha+1}} e^{-z^{-\alpha}}, \quad z \in [0, \infty). \quad (10)$$

Here one can identify $a_N = 0$, $b_N = (AN/\alpha)^{1/\alpha}$. This is the famous *Fréchet* distribution.

B. Parent distributions with a faster than power law tail

We consider the parent distributions with tails that decay faster than a power law, but are still unbounded, such as $p(x) \sim e^{-x^\delta}$ with $\delta > 0$. In this case, one finds the scaling function to be

$$F_2(z) = e^{-e^{-z}}, \quad (11)$$

where the PDF is given by

$$f_2(z) = F_2'(z) = e^{-z-e^{-z}}, \quad z \in (-\infty, \infty). \quad (12)$$

This is the famous *Gumbel* distribution [1, 2]. Here one finds $a_N = (\ln N)^{1/\delta}$, $b_N = \frac{1}{\delta} (\ln N)^{1/\delta - 1}$. Since a_N is the typical value of the maximum and is defined by

$$N \int_{a_N}^{\infty} p(y) dy = 1, \quad (13)$$

we see from Eq. (7) that the weight will be to the right of a_N , since $F_2(z)$ in Eq. (11) decays extremely rapidly to 0 for negative argument. In the following we will compute the scaling functions for the parent distributions having the exponential and the Gaussian tails.

1. The exponential case $p(x) = e^{-x}$ for $x \geq 0$

In this case, applying the form of $p(x)$, one finds

$$Q_N(x) = [1 - e^{-x}]^N = e^{N \log[1 - e^{-x}]} \sim e^{-Ne^{-x}} = e^{-e^{-(x - \log N)}} = F_2(z) \quad (14)$$

with $z = x - \log N$ and the following identification $a_N = \ln N$, $b_N = 1$ in Eq. (7).

2. The Gaussian case $p(x) = \frac{1}{\sqrt{2\pi}} e^{-x^2/2}$

As in the previous example, substituting this form of $p(x)$ in Eq. (6) we obtain

$$Q_N(x) = \left[1 - \frac{1}{2} \operatorname{erfc} \left(\frac{x}{\sqrt{2}} \right) \right]^N = \exp \left[N \ln \left(1 - \frac{1}{2} \operatorname{erfc} \left(\frac{x}{\sqrt{2}} \right) \right) \right], \quad (15)$$

where $\operatorname{erfc}(x) = \frac{2}{\sqrt{\pi}} \int_x^\infty e^{-y^2} dy$ is the complementary error function. Expanding the logarithm in Taylor series for large x , we get an approximate formula

$$Q_N(x) \approx \exp \left[-\frac{N}{2} \operatorname{erfc} \left(\frac{x}{\sqrt{2}} \right) \right]. \quad (16)$$

We only want to retain the leading behaviour for large x . This can be done by using the large x behaviour of $\operatorname{erfc}(x)$ which has the following form

$$\operatorname{erfc}(x) \approx \frac{e^{-x^2}}{x\sqrt{\pi}}, \quad x \rightarrow \infty. \quad (17)$$

Finally, using this asymptotic behaviour in Eq. (16), we get, for both N and x large (note that we still have not taken the scaling limit yet) the leading behaviour

$$Q_N(x) \approx \exp \left(-\frac{N}{\sqrt{2\pi}} \frac{e^{-x^2/2}}{x} \right). \quad (18)$$

To cast this tail behavior in the universal form as in Eq. (7), we look for a_N and b_N such that $(x - a_N)/b_N = z$ is fixed as $N \rightarrow \infty$. For this, we set $x = a_N + b_N z$ in Eq. (18) to get

$$Q_N(x = a_N + b_N z) \approx \exp \left[-\frac{N}{\sqrt{2\pi}} \frac{1}{(a_N + b_N z)} e^{-\frac{1}{2}(a_N^2 + 2a_N b_N z + b_N^2 z^2)} \right]. \quad (19)$$

Let us anticipate (and verify a posteriori) that $b_N \ll a_N$ such that $(a_N + b_N z) \approx a_N$ to leading order and furthermore we can drop the term $b_N^2 z^2$ inside the exponential, since we expect it to be small. We then choose a_N and b_N such that

$$\frac{N}{\sqrt{2\pi} a_N} e^{-\frac{a_N^2}{2}} = 1, \quad \text{and} \quad a_N b_N = 1. \quad (20)$$

With this choice of a_N and b_N we then have

$$Q_N(x = a_N + b_N z) \approx e^{-e^{-z}} = F_2(z). \quad (21)$$

The centring and the scaling constants a_N and b_N can be obtained for large N from Eq. (20). To leading order, one gets

$$a_N \approx \sqrt{2 \ln N} - \frac{\ln(\ln N)}{2\sqrt{2 \ln N}} + \dots \quad \text{and} \quad b_N = \frac{1}{a_N}. \quad (22)$$

Thus we see that, even though the finite N formula of $Q_N(x)$ in Eq. (6) for the two distributions $p(x) = e^{-x}$ (with $x \geq 0$) and $p(x) = \frac{1}{\sqrt{2\pi}} e^{-x^2/2}$ look rather different from each other at first glance, once we center and scale by appropriate a_N and b_N which differ in the two cases, the scaling function for the two cases is exactly identical and is given by the Gumbel law $F_2(z) = e^{-e^{-z}}$.

One can now generalize the Gaussian case to any distribution with a large x tail $p(x) \sim C e^{-x^\delta}$ with $C, \delta > 0$. In this case, one can carry out a straightforward large N analysis of the formula in Eq. (6), following the same method as discussed above. The centring factor a_N and the width b_N in Eq. (7) are given, for large N , by

$$a_N \approx (\ln N)^{1/\delta} \quad , \quad b_N \approx \frac{1}{\delta} (\ln N)^{1/\delta-1} . \quad (23)$$

The limiting scaling function however remains the Gumbel form $F_2(z) = e^{-e^{-z}}$ for any $\delta > 0$. Interestingly, the width b_N of the maximum distribution around its peak at a_N increases for large N for $0 < \delta < 1$, while it decreases for large N for $\delta > 1$. Thus, for $0 < \delta < 1$, the PDF of the maximum becomes broader and broader with increasing N , while, for $\delta > 1$, the PDF becomes narrower and narrower around its peak.

C. Parent distributions with an upper bounded support

We now consider the parent distributions with bounded tails such as $p(x) \xrightarrow{x \rightarrow a} (a-x)^{\beta-1}$ with $\beta > 0$. In this case

$$F_3(z) = \begin{cases} e^{-(-z)^\beta} & \text{for } z \leq 0 \\ 1 & \text{for } z \geq 0 . \end{cases} \quad (24)$$

The PDF is therefore given by

$$f_3(z) = \beta(-z)^{\beta-1} e^{-(-z)^\beta}, \quad z \in (-\infty, 0] , \quad (25)$$

which is the well-known *Weibull* distribution. Note that in the case where $p(x)$ vanishes faster than a power law at the upper bound, for instance if it has an essential singularity $p(x) \sim e^{-1/(a-x)^\nu}$ with $\nu > 0$, then the limiting distribution of the maximum is given by a Gumbel law (11).

Let us now summarize the results for the limiting distribution of the maximum for IID random variables in the following table.

Parent distribution $p(x)$	Scaling function $F(z)$	PDF of maximum $f(z)$	Nomenclature
$x^{-(1+\alpha)}$; $\alpha > 0$	$e^{-z^{-\alpha}} \theta(z)$	$\frac{\alpha}{z^{\alpha+1}} e^{-z^{-\alpha}}$; $z > 0$	Fréchet
e^{-x^δ}	$e^{-e^{-z}}$	$e^{-z-e^{-z}}$	Gumbel
$(a-x)^{\beta-1}$; $\beta > 0$	$e^{-(-z)^\beta} \theta(-z) + \theta(z)$	$\beta(-z)^{\beta-1} e^{-(-z)^\beta}$; $z < 0$	Weibull

So far, we discussed about the limiting laws in the limit of large sample size N . It turns out however that the convergence to these limiting laws is extremely slow and in simulations and experiments, it is very hard to see these limiting distributions [82, 83]. A renormalization group treatment has been developed that describes how these EVS distributions for IID variables approach their limiting ‘‘fixed point’’ distributions. Interested readers may consult Refs. [82, 84–87].

In the discussion above, we have only considered the limiting large N distributions that describe the *typical* fluctuations of the maximum value around its mean, i.e., when $x \sim a_N + b_N z$ where $z = \mathcal{O}(1)$. However, *atypical* fluctuations much larger than this typical scale, i.e., when $|z| \gg 1$, are not described by these limiting distributions, but rather by appropriate large deviation tails (for a recent discussion see [88]).

D. Order statistics

An interesting generalization of the statistics of the global maximum corresponds to studying the statistics of successive maxima, known as the ‘order’ statistics [89, 90]. For a recent review on order statistics, see [57]. Consider again the set of IID random variables $\{x_1, x_2, \dots, x_N\}$ and arrange them in decreasing order of their values. So, if we denote them by $M_{k,N}$ where k is the order and N is the number of variables, then

$$\begin{aligned} M_{1,N} &= \max(x_1, x_2, \dots, x_N) , \\ M_{2,N} &= \text{second max}(x_1, x_2, \dots, x_N) , \\ &\vdots \\ M_{k,N} &= k\text{-th max}(x_1, x_2, \dots, x_N) , \\ &\vdots \\ M_{N,N} &= \min(x_1, x_2, \dots, x_N) , \end{aligned} \quad (26)$$

and henceforth by definition $M_{1,N} > M_{2,N} > \dots > M_{N,N}$. It is of interest to study the statistics of the k -th maximum $M_{k,N}$ and the statistics of the gap defined by $d_{k,N} = M_{k,N} - M_{k+1,N}$. As before, we consider the parent distribution to be $p(x)$. Then we define the upward and the downward cumulative distributions respectively

$$p_{>}(x) = \int_x^{\infty} p(y) dy, \quad (27)$$

$$p_{<}(x) = \int_{-\infty}^x p(y) dy. \quad (28)$$

Then the cumulative probability $Q_{k,N}(x)$ that the k -th maximum stays below x is given by

$$Q_{k,N}(x) = \text{Prob}[M_{k,N} \leq x] = \sum_{m=0}^{k-1} \binom{N}{m} [p_{>}(x)]^m [p_{<}(x)]^{N-m}, \quad (29)$$

where m is the number of points above x . The exact PDF is then given by

$$P_{k,N} = \text{Prob}[M_{k,N} = x] = N \binom{N-1}{k-1} p(x) [p_{<}(x)]^{N-k} [p_{>}(x)]^{k-1}. \quad (30)$$

With some more work, one can also obtain the probability distribution of the gap $d_{k,N} = M_{k,N} - M_{k+1,N}$ as (see e.g. [57])

$$P_{k,N}(d) = \text{Prob}[d_{k,N} = d] = N(N-1) \binom{N-2}{k-1} \int_{-\infty}^{\infty} dx p(x) p(x-d) [p_{<}(x)]^{N-k-1} [p_{>}(x)]^{k-1}. \quad (31)$$

As for the cumulative distribution of the maximum, we can again do the same analysis as before and extract the leading large N behavior. One finds [57, 89, 90]

$$Q_{k,N}(x) = \text{Prob}[M_{k,N} \leq x] \xrightarrow[z=(x-a_N)/b_N \text{ fixed}]{x \rightarrow \infty, N \rightarrow \infty} G_k \left(\frac{x - a_N}{b_N} \right), \quad (32)$$

where the scaling function $G_k(z)$ is given by

$$G_k(z) = F_{\mu}(z) \sum_{j=0}^{k-1} \frac{[-\ln F_{\mu}(z)]^j}{j!} = \frac{1}{\Gamma(k)} \int_{-\ln F_{\mu}(z)}^{\infty} e^{-t} t^{k-1} dt, \quad (33)$$

where $F_{\mu}(z)$, with $\mu = 1, 2, 3$, denote respectively the Fréchet, Gumbel and Weibull scaling functions discussed above respectively in Eqs. (9), (11) and (24). In particular setting $k = 1$ (global maximum) in Eq. (33) one recovers $G_1(z) = F_{\mu}(z)$, as expected. As an example, if we choose the parent distribution $p(x)$ from the subclass B where $F_2(z) = e^{-e^{-z}}$ is the Gumbel distribution, we find $G_k(z) = e^{-e^{-z}} \sum_{j=0}^{k-1} \frac{e^{-jz}}{j!}$ and the PDF is $G'_k(z) = \frac{e^{-kz - e^{-z}}}{(k-1)!}$. This is often known as the generalized Gumbel law. Similarly, one can also derive the limiting scaling distributions of the k -th gap, $d_{k,N} = M_{k,N} - M_{k+1,N}$ (see Ref. [57] for more details).

IV. CORRELATED RANDOM VARIABLES

In this section we study the extreme statistics of correlated random variables. In the first subsection we revisit the random variables where the correlations are weak and then we study the “strongly” interacting random variables. There is no general framework to study the statistics of the correlated random variables. However, we show in the following that for weakly correlated variables, one can provide a rather general renormalization group type of argument to study the extreme statistics. This argument does not work when the variables are strongly correlated and one has to study case by case different models to gain an insight.

A. Weakly correlated random variables

Suppose that we have a set of random variables that are not independent, but correlated such that the connected part of the correlation function decays fast (say exponentially) over a certain finite correlation length ξ (see Fig. 1)

$$C_{i,j} = \langle x_i x_j \rangle - \langle x_i \rangle \langle x_j \rangle \sim e^{-|i-j|/\xi}. \quad (34)$$

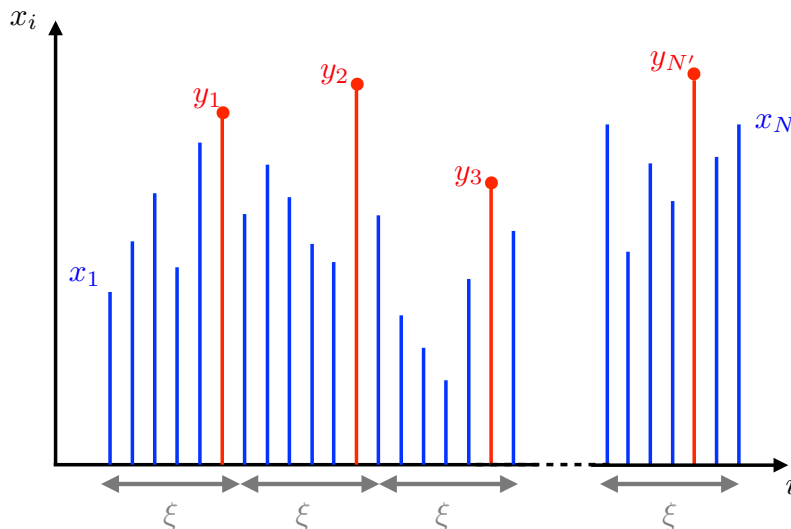


FIG. 1. Block decomposition of the system. The system is divided into blocks of size ξ . The total size of the system is N , and the number of blocks is $N' = N/\xi$. The local maximum in each block is denoted by y_i . The variables y_i 's are thus essentially uncorrelated. Hence, we have

$$M = \max[x_1, x_2, \dots, x_N] = \max[y_1, y_2, \dots, y_{N'}]. \quad (35)$$

Therefore, in principle if one knows the PDF of the y_i 's, then this problem is essentially reduced to calculating the maximum of N' uncorrelated random variables $\{y_1, y_2, \dots, y_{N'}\}$, which has already been discussed before. So, we know that depending on the tail of $p(y)$, the limiting distribution of M of N weakly correlated variables will, for sure, belong to one of the three (Fréchet, Gumbel or the Weibull class) limiting extreme distributions of IID random variables. To decide the tail of $p(y)$, of course one needs to solve a *strongly* correlated problem since inside each block the variables are strongly correlated. However, one can often guess the tail of $p(y)$ without really solving for the full PDF of $p(y)$ and then one knows, for sure, to which class the distribution of the maximum belongs to. As a concrete example of this procedure for weakly correlated variables, we discuss in the next section the Ornstein-Uhlenbeck stochastic process where one can compute the EVS exactly and demonstrate that indeed this heuristic renormalization group argument works very well. Note also that, in the case of Gaussian random variables x_i 's with stationary correlations, i.e. $C_{i,j} = c(|i-j|)$ in Eq. (34), one can show [91] that if $c(x)$ decays faster than $1/\ln(x)$ for large x , then the distribution of x_{\max} is still given by a Gumbel distribution.

To summarize, the problem of EVS of weakly correlated random variables basically reduces to IID variables with an effective number $N' = N/\xi$ where ξ is the correlation length. So, the real challenge is to compute the EVS of strongly correlated variables where $\xi \geq O(N)$, to which we now turn to below.

B. Strongly correlated random variables

Strongly correlated means that the correlation length prevails over the whole system such that the idea of block spins as in Fig. 1 will no longer hold. A general theory for calculating the EVS, such as in case of IID or weakly correlated variables, is currently lacking for such strongly correlated variables. In the absence of a general theory, one

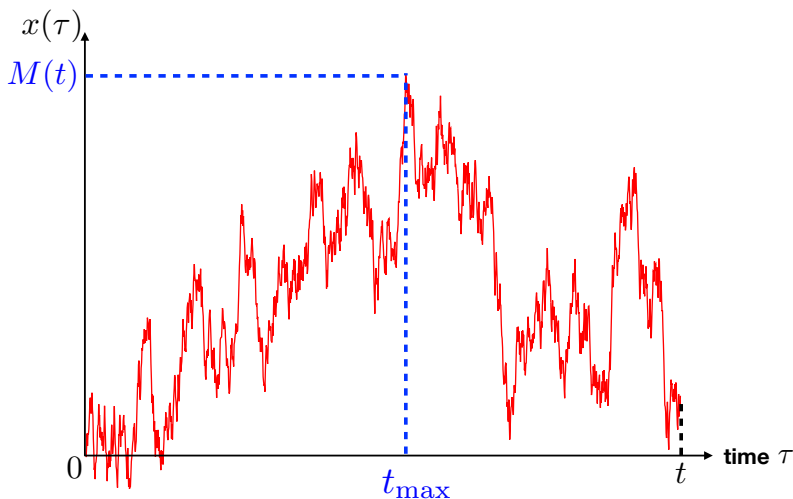


Figure 2: Plot of the maximum $M(t)$ of a process $x(\tau)$ over the time window $[0, t]$.

tries to study different exactly solvable special cases in the hope of gaining some general insights. There are examples, though their numbers are unfortunately few, where the EVS of a strongly correlated system can be computed exactly. In the following, we will discuss a few examples of such exactly solvable cases.

As a first example of a strongly correlated system, we will consider the one-dimensional Brownian motion, for which the distribution of maximum can be computed explicitly. Next, we will discuss the Ornstein-Uhlenbeck (OU) process, which represents the noisy motion of a classical particle in a harmonic well. We will see that the OU process actually represents a weakly correlated system, for which one can compute the distribution of the maximum explicitly, demonstrating the power of the heuristic argument presented in the previous subsection for weakly correlated variables. Next, we will discuss the case of EVS of random variables subjected to a global constraint, like the famous *zero-range* process, and then the case of hierarchically and logarithmically correlated variables. We will then turn to the EVS in stochastic resetting systems, after which we will present the problem of the maximum height distribution of a fluctuating $(1 + 1)$ -dimensional interface in its stationary state. Finally, we will discuss the statistics of the largest eigenvalue for Gaussian random matrices.

1. One-dimensional Brownian motion and random walks

We consider the case where the random variables x_i 's represent the positions of a one-dimensional random walker at discrete time-step i , starting from $x_0 = 0$. We are interested in the maximum position of the walker up to step n . Even though the discrete problem can be solved explicitly (see the discussion below), for simplicity we will first consider below the continuous-time version of the random walk, i.e., a one-dimensional Brownian motion whose position $x(\tau)$ evolves via the stochastic Langevin equation

$$\frac{dx}{d\tau} = \eta(\tau), \quad (36)$$

starting from $x(0) = 0$ and $\eta(\tau)$ represents a Gaussian white noise with zero mean $\langle \eta(\tau) \rangle = 0$ and delta-correlations $\langle \eta(\tau)\eta(\tau') \rangle = 2D \delta(\tau - \tau')$. We are interested in the PDF of the maximum $M(t)$ of this Brownian motion $x(\tau)$ over the time window $[0, t]$ (see Fig. 2)

$$M(t) = \max_{0 \leq \tau \leq t} [x(\tau)]. \quad (37)$$

To proceed, we first note that $x(\tau) = \int_0^\tau \eta(s) ds$ and hence, one can easily compute the mean and the correlator of the process $x(\tau)$: $\langle x(\tau) \rangle = 0$ and $\langle x(\tau)x(\tau') \rangle = 2D \min(\tau, \tau')$. Thus the variables $x(\tau)$ at different times are strongly correlated. The correlation function does not decay and persists over the whole sample size $\tau \in [0, t]$.

As done in the IID case [see Eq. (4)] it is also very useful here to define the cumulative distribution of the maximum

$$Q(z, t) = \text{Prob}[M(t) \leq z] = \text{Prob}[x(\tau) \leq z, 0 \leq \tau \leq t]. \quad (38)$$

First, we notice that $Q(z, t) = 0$ for $z < 0$ since $M(t) \geq x(0) = 0$. To compute $Q(z, t)$ for $z \geq 0$, we note that it just represents the probability that the Brownian particle, starting at $x(0) = 0$, stays below the level z up to time t . Let $P(x, t|z)$ denote the probability density for the particle to reach x at time t , while staying below the level z during $[0, t]$. It is then easy to see that $P(x, t|z)$ satisfies the diffusion equation in the semi-infinite domain $x \in (-\infty, z]$

$$\frac{\partial P}{\partial t} = D \frac{\partial^2 P}{\partial x^2}, \quad (39)$$

with the following initial and boundary conditions

$$P(x, 0|z) = \delta(x),$$

and $P(x \rightarrow -\infty, t|z) = 0, P(x = z, t|z) = 0.$ (40)

The absorbing boundary condition $P(x = z, t|z) = 0$ at $x = z$ guarantees that the particle does not cross the level at $x = z \geq 0$. The solution is simple and can be obtained by the method of images [92–94]

$$P(x, t|z) = \frac{1}{\sqrt{4\pi Dt}} [e^{-\frac{x^2}{4Dt}} - e^{-\frac{(x-2z)^2}{4Dt}}]. \quad (41)$$

Therefore the cumulative distribution function of the maximum is given by (for $z \geq 0$)

$$Q(z, t) = \int_{-\infty}^z dx P(x, t|z) = \text{erf}\left(\frac{z}{\sqrt{4Dt}}\right); \text{ where } \text{erf}(z) = \frac{2}{\sqrt{\pi}} \int_0^z e^{-u^2} du, \quad (42)$$

(43)

while we recall that $Q(z, t) = 0$ for $z < 0$. Hence the PDF $P_M(z, t)$ of $M(t)$ is given by

$$P_M(z, t) = \frac{\partial Q(z, t)}{\partial z} = \theta(z) \frac{1}{\sqrt{\pi Dt}} e^{-\frac{z^2}{4Dt}}, \quad (44)$$

where $\theta(z)$ is the Heaviside theta function, i.e. $\theta(z) = 1$ if $z > 0$ and $\theta(z) = 0$ if $z < 0$. In particular, from Eq. (44), one easily computes the expected maximum $\langle M(t) \rangle = \frac{2}{\sqrt{\pi}} \sqrt{Dt}$. This thus represents, perhaps, the simplest example of a strongly correlated system for which one can compute the distribution of the maximum exactly.

In fact various other extreme observables can be computed for Brownian motion and its variants (like the Brownian bridge, which is the BM conditioned to start and end at the origin at time t , or the Brownian excursion, which is a Brownian bridge conditioned, additionally, to stay positive on $[0, t]$). This includes for instance the temporal correlations of the (running) maximum [95, 96], the time t_{\max} (see Fig. 2) at which the BM or its variants reaches its maximum $M(t)$ [38, 52, 97] (see section IV C 2 below for a more complete discussion of this observable) as well as other functionals of $M(t)$ [98, 99]. These extremal properties of BM have found several interesting applications like in the statistics of the convex hull of *two-dimensional* BM [45, 48, 49], in enumerative combinatorics and computer science [98–102] as well as in the study of fluctuating interfaces [23, 24], which we will discuss further below. EVS have also been studied for more general stochastic processes (i.e. beyond Brownian motion and its variants) involving (i) either a single degree of freedom, like the so called continuous time random walks (CTRW) [52, 103], the random acceleration process [34, 50] and more general $1/f^\alpha$ noise [27, 104, 105] as well as fractional Brownian motion [106–110] (ii) or several degrees of freedom like N independent [111, 112] as well as non-intersecting Brownian motions [41–44, 53, 58, 59, 61, 113–115] and branching Brownian motions [63, 116–124]. Extreme value questions for these processes have recently found many applications ranging from the number of common and distinct visited sites by N random walkers [112], distribution of the cover time by N Brownian motions on an interval of length L [144] and the distribution of the cover time of a single transient walker in higher dimensions [126], combinatorics [41, 42, 44], fluctuating interfaces in the Kardar-Parisi-Zhang universality class [42, 53, 58, 61, 62], disordered systems [116, 117], genetics [118], propagation of epidemics [63] or in random planar geometry [127–129].

All these properties discussed so far in this section concern continuous time processes, but one can also study extreme value questions for discrete time processes, like random walks on the real line mentioned in the introduction of this section. In this case, at each time step, the walker performs a jump η whose size is a random variable drawn from a jump PDF $f(\eta)$. The position of the walker x_n thus evolves according to the Markov dynamics

$$x_n = x_{n-1} + \eta_n, \quad (45)$$

starting from a given initial position x_0 . In Eq. (45) the η_n 's are IID random variables distributed according to $f(\eta)$. The RW model (45) includes discrete random walks (RWs), e.g. $f(\eta) = (1/2)\delta(\eta - 1) + (1/2)\delta(\eta + 1)$, as well as RWs with continuous jump distributions, such as a uniform, a Gaussian or a Cauchy distribution for instance. One

usually distinguishes between two different types of RWs: (i) the “standard” RWs, for which $\sigma^2 = \langle \eta^2 \rangle - \langle \eta \rangle^2$ is finite, which converge after a large number of steps to the Brownian motion as in Eq. (36) and (ii) the Lévy flights, for which σ is infinite, which is the case for heavy tailed distributions $f(\eta) \propto |\eta|^{-1-\mu}$ for large $|\eta|$, with a so-called Lévy index $0 < \mu < 2$ (for instance, a Cauchy jump distribution corresponds to $\mu = 1$). For large n , the extreme value properties of the standard RWs coincide at leading order with that of the BM studied above while they are quite different for the Lévy flights. Unlike the Brownian motion which is continuous both in space and time, the study of EVS for RWs and Lévy flights is usually much harder. Nevertheless, there is now an important literature on this subject and a lot of results are now available [57, 93, 94, 130–135], which are useful for instance for discrete height model [76], in computer science (e.g., for packing problems in two-dimensions [136]) or to characterize the convex hull of two-dimensional random walks [137]. Interestingly, for discrete-time RWs and Lévy flights described by Eq. (45), one can study the statistics not only of the global (of first) maximum $M(n)$ but also of the second, third, ..., more generally of the k -th maximum, as done previously in the IID case [see Eq. (26)]. Of particular interest in this context are the gaps between two successive maxima and for which a lot of results have been obtained during the last years [104, 138–145].

2. Ornstein-Uhlenbeck (OU) process

We now consider a Brownian particle in a harmonic potential governed by the following Langevin equation

$$\frac{dx}{d\tau} = -\mu x + \eta(\tau) , \quad (46)$$

where, as before, $\eta(\tau)$ is a Gaussian white noise with zero mean and is delta correlated, $\langle \eta(\tau)\eta(\tau') \rangle = 2D\delta(\tau - \tau')$. Assuming that the particle starts at the origin $x(0) = 0$, $x(\tau)$ is a Gaussian random variable of zero mean at all time $\tau \geq 0$ (since its equation of evolution (46) is linear). It is thus fully characterized by its two-time correlation function $C(t_1, t_2)$ which can be easily computed as

$$C(t_1, t_2) = \langle x(t_1)x(t_2) \rangle = \frac{D}{\mu} [e^{-\mu|t_1-t_2|} - e^{-\mu(t_1+t_2)}] . \quad (47)$$

Clearly the correlation function reduces to the Brownian limit when $\mu \rightarrow 0$, since in this limit $C(t_1, t_2) \rightarrow 2D \min(t_1, t_2)$ and the system becomes strongly correlated. In contrast, for nonzero $\mu > 0$, the correlation function, at large times $t_1, t_2 \gg 1/\mu$, decays exponentially with the time-difference $C(t_1, t_2) \approx \frac{1}{2\mu} e^{-\mu|t_1-t_2|}$ with a correlation length $\xi = 1/\mu$. From our above arguments about weakly correlated random variables (see Section IV A), we would then expect to get the limiting Gumbel distribution for $\mu > 0$ (since $x(\tau)$ is a Gaussian random variable of variance $\sqrt{D/\mu}$ for large τ). We demonstrate below how this Gumbel distribution emerges by solving exactly the EVS for the OU process.

As before, let $Q(z, t)$ denote the cumulative distribution of the maximum $M(t)$ of the OU process in the time interval $[0, t]$. The particle starts at the origin $x(0) = 0$ and evolves via Eq. (46). Let $P(x, t|z)$ denote the probability density for the particle to arrive at x at time t , while staying below the level z . This restricted propagator satisfies the Fokker-Planck equation in the domain $x \in (-\infty, z]$

$$\frac{\partial P}{\partial t} = D \frac{\partial^2 P}{\partial x^2} + \mu \frac{\partial}{\partial x} (xP) , \quad (48)$$

with the initial condition $P(x, 0|z) = \delta(x)$ and the boundary conditions $P(x, t|z) = 0$ as $x \rightarrow -\infty$ together with the absorbing condition at level z , i.e. $P(x = z, t|z) = 0$ for all t . For simplicity, we will set $D = 1/2$. We note that, unlike in the Brownian case ($\mu = 0$), for $\mu > 0$ we can no longer use the method of images due to the presence of the potential. However, one can solve this equation by the eigenfunction expansion and the solution can be expressed as

$$P(x, t|z) = \sum_{\lambda} a_{\lambda} e^{-\lambda t} D_{\lambda/\mu}(-\sqrt{2\mu}x) e^{-\mu x^2/2} \quad (49)$$

where $D_p(z)$ is the parabolic cylinder function which satisfies the second order ordinary differential equation: $D_p''(z) + (p + 1/2 - z^2/4) D_p(z) = 0$ (out of the two linearly independent solutions, we choose the one that vanishes as $z \rightarrow \infty$). The absorbing boundary condition $P(x = z, t|z) = 0$ induces the boundary condition on the eigenfunction

$$D_{\lambda/\mu}(-\sqrt{2\mu}z) = 0 , \quad (50)$$

which then fixes the eigenvalues λ 's, which are necessarily positive. Finally, in Eq. (49) the a_λ 's can be computed explicitly

$$a_\lambda = \frac{\sqrt{2\pi\mu} 2^{\frac{\lambda}{2\mu}}}{\Gamma\left(\frac{1-\lambda/\mu}{2}\right) c_\lambda}, \quad c_\lambda = \int_{-\infty}^{\infty} D_{\lambda/\mu}^2(x) e^{-x^2/2} dx. \quad (51)$$

At large times t , the summation in Eq. (49) is dominated by the term involving the smallest eigenvalue $\lambda_0(z)$, which evidently depends on z . For arbitrary z , it is difficult to solve $D_{\lambda/\mu}(-\sqrt{2\mu}z) = 0$ and determine the smallest eigenvalue $\lambda_0(z)$. However, for large z , one can make progress by perturbation theory and one can show that to leading order for large z ,

$$\lambda_0(z) \xrightarrow{z \rightarrow \infty} \frac{1}{\sqrt{\pi}} \mu^{3/2} z e^{-\mu z^2}, \quad (52)$$

while $a_{\lambda_0} \rightarrow a_0 = \sqrt{2\mu/\pi}$ (note also that $D_0(x) = e^{-x^2/4}$). Consequently, for large t and large z ,

$$\begin{aligned} Q(z, t) &\sim e^{-\lambda_0(z)t} \sim e^{-e^{-\mu z^2 + \log\left(\frac{t\mu^{3/2}z}{\sqrt{\pi}}\right)}} \\ &\rightarrow F_2\left[\sqrt{4\mu \ln t} \left(z - \frac{1}{\sqrt{\mu}} \sqrt{\ln t}\right)\right], \end{aligned} \quad (53)$$

where $F_2(y) = \exp[-\exp[-y]]$ is the Gumbel distribution. As a result, for $\mu > 0$, the average value of the maximum grows very slowly for large t as, $\langle M(t) \rangle \sim \frac{1}{\sqrt{\mu}} \sqrt{\ln t}$, while its width around the mean decreases as $\sim 1/\sqrt{\ln t}$. In fact, for $\mu > 0$, a full analysis of the mean value of the maximum $\langle M(t) \rangle$ for all t shows that initially it grows as \sqrt{t} (for $t \ll 1/\mu$) where it does not feel the confining potential and hence behaves as a Brownian motion. But for $t \gg 1/\mu$, the particle feels the potential and the mean maximum crosses over to a slower growth as $\sqrt{\ln t}$. Hence, one has

$$\langle M(t) \rangle \sim \begin{cases} \sqrt{t} & \text{for } t \ll 1/\mu \\ \sqrt{\ln t} & \text{for } t \gg 1/\mu, \end{cases} \quad (54)$$

which indicates a crossover from a strongly correlated regime at short time $t \ll 1/\mu$ to an IID regime at longer time $t \gg 1/\mu$.

3. Extreme statistics in the presence of a global constraint

Another interesting example of a correlated system is when the correlations emerge due to the presence of a global conservation law for the dynamics of the underlying random variables. There are several examples of this that we briefly discuss here.

The first example concerns a well known interacting particle systems known as the zero range process (ZRP) [146, 147] where one considers a one-dimensional lattice of N sites with periodic boundary condition. At each site, there is a certain number of particles $\ell_i \geq 0$. From the i -th site, a single particle hops to a neighbouring site with a rate $U(\ell_i)$ that depends only on the occupation number of the departure site, provided $\ell_i > 0$. Clearly, the dynamics conserves the total number of particles $\sum_{i=1}^L \ell_i = L$. At long times, the system reaches a stationary state where the joint distribution of the occupation numbers at different sites is given by

$$P_{\text{ZRP}}(\ell_1, \dots, \ell_N | L) = \frac{1}{Z_N(L)} \prod_{i=1}^N f(\ell_i) \delta_{\sum_{i=1}^N \ell_i, L}, \quad (55)$$

where $f(\ell) = 1/\prod_{k=1}^{\ell} U(k)$ and $Z_N(L)$ is the normalization constant. The δ -function in (55) enforces the global constraint that the number of particles L is fixed. Without this δ -function, the joint distribution would factorize and we would be back to the IID case. However, the presence of this δ -function makes these variables correlated. We are interested in the extreme statistics, i.e. the statistics of $\ell_{\max} = \max_{1 \leq i \leq N} \ell_i$. This corresponds to the largest number of particles carried by a single site, out of N sites. Of particular physical interest is the case when the transfer rate function $U(k)$ is such that the steady state weight function has a tail such that $e^{-c\ell} \ll f(\ell) \ll 1/\ell^2$ for large ℓ , where c is any arbitrary constant [147]. A well studied example is the case when $f(\ell)$ has a power law tail, $f(\ell) \sim A/\ell^\gamma$ for large ℓ , with $\gamma > 2$ and $A > 0$. In this case, it is known that a condensation transition happens when the density $\rho = L/N$ exceeds a certain critical value ρ_c . For $\rho < \rho_c$ the particles are ‘‘democratically’’ distributed among all sites:

this is the “fluid” phase. For $\rho > \rho_c$ a single condensate site emerges that carries a finite fraction of the total number of particles: this is the “condensed” phase. Clearly, in this condensed phase, ℓ_{\max} is identified with the number of particles carried by this single condensate.

This ZRP is one example where, despite the presence of correlations, the statistics of ℓ_{\max} can be computed explicitly, in the limit of large N , large L , but with the density $\rho = L/N$ fixed [36]. Let us summarize the main results. For any fixed $\gamma > 2$, one finds that the center and scaled distribution of ℓ_{\max} , in the fluid phase $\rho < \rho_c$, converges to the Gumbel distribution discussed before in Section III. In this case, the global constraint enforced by the δ -function can be relaxed (akin to canonical to grand-canonical) and one can replace it in Eq. (55) by $e^{-\mu \sum_{i=1}^N \ell_i}$ where $\mu > 0$ is the chemical potential (or Lagrange multiplier). This factorizes the joint distribution in Eq. (55) into a product of effective IID random variables with an effective distribution $f_{\text{IID}}(\ell) = f(\ell)e^{-\mu\ell}$. Thus, for $\mu > 0$, the distribution of these IID variables has an effective exponential tail and, hence, the distribution of their maximum converges to the Gumbel distribution, as discussed in Section III. Note that this exponential tail is induced here by the global constraint. When ρ approaches ρ_c from below, $\mu \rightarrow 0$ and we again obtain a factorization of the joint distribution in Eq. (55) but now the effective distribution has a power law tail $f(\ell) \sim A/\ell^\gamma$ for large ℓ . Consequently, the distribution of the maximum, centred and scaled, approaches the Fréchet distribution, as discussed in Section III, thus as if the global constraint does not play any role at all at the critical point $\rho = \rho_c$. However, for $\rho > \rho_c$, it turns out that the global constraint has a much stronger effect and the scaled distribution of ℓ_{\max} has a non-trivial distribution given by [36]

$$\text{Prob.}(\ell_{\max} = x, N) \sim \frac{1}{N^\delta} V_\gamma \left(\frac{x - (\rho - \rho_c)N}{N^\delta} \right), \quad (56)$$

where the exponent δ is given by

$$\delta = \begin{cases} \frac{1}{\gamma-1}, & 2 < \gamma < 3, \\ 1/2, & \gamma > 3. \end{cases} \quad (57)$$

The scaling function $V_\gamma(z)$ also depends on γ . While for $\gamma > 3$ it is a simple Gaussian, for $2 < \gamma < 3$, it has a non-trivial form given by the integral representation

$$V_\gamma(z) = \int_{-i\infty}^{+i\infty} \frac{ds}{2\pi i} e^{-zs+bs^{\gamma-1}}, \quad (58)$$

where $b = A\Gamma(1 - \gamma)$ with A being the amplitude of the power law tail of $f(\ell) \sim A/\ell^\gamma$ for large ℓ . This therefore represents an example where correlations affect the extreme value distribution non-trivially and yet remains computable.

Another example with a global constraint concerns the largest time interval between returns to the origin of a one-dimensional lattice random walk [148] and more generally a renewal process [149, 150]. In this case, let ℓ_i denote the time interval between the i -th and the $(i - 1)$ -th return to the origin of a random walk of L steps. After every return to the origin, the process gets renewed due to the Markov nature of the walk. Consequently, the joint PDF of the intervals between successive returns and the total number of intervals N in L steps is given by

$$P_{\text{REN}}(\ell_1, \dots, \ell_N, N|L) \propto \left[\prod_{n=1}^{N-1} f(\ell_n) \right] q(\ell_N) \delta_{\sum_{n=1}^N \ell_n, L}, \quad (59)$$

where L represents the total time interval. Here the number of intervals N is also a random variable, unlike in the ZRP case (55) where N was fixed. In addition, at variance with Eq. (55), while the first $N - 1$ intervals in Eq. (59) have the same weight $f(\ell_n)$, the last one has a different weight $q(\ell_N) = \sum_{\ell=\ell_N+1}^{\infty} f(\ell)$ (this is due the fact that the last interval is yet to be renewed). In these renewal processes (59), the weight $f(\ell)$ is taken as an input in the model. For example, for a $1d$ -random walk, $f(\ell) \sim 1/\ell^{3/2}$ for large ℓ . The statistics of $\ell_{\max} = \max_{1 \leq i \leq N} \ell_i$ has been studied in detail in Refs. [149, 150]. The main results can be summarized as follows. If $f(\ell)$ decays faster than $1/\ell^2$ for large ℓ , one essentially recovers the IID results for the distribution of ℓ_{\max} , indicating that the global constraint does not play any significant role. However, for $f(\ell) \sim 1/\ell^\gamma$ with $1 < \gamma < 2$, the constraint significantly modifies the distribution of ℓ_{\max} , leading to a nontrivial distribution [150]. In addition, in Refs. [149, 150], another extreme observable was studied, namely the probability that the last interval is the longest.

We finish this section with yet another example of extreme statistics in the presence of a global constraint. It appeared in a recently introduced truncated long-ranged Ising model in a one-dimensional lattice of size L , where the couplings between two spins at sites i and j decay as an inverse square law, provided both spins belong to the same

domain. The spins across domains do not have any long range interaction [151, 152]. In addition to this long-range interaction, there is also a short-range interaction between neighboring spins. This model was shown to exhibit a mixed order phase transition (MOT) at a finite critical temperature where the correlation length diverges, as in a second order phase transition, but the order parameter undergoes a jump as in a first order phase transition. The configurations of the system can be labelled by the lengths of spin domains $\{\ell_i\}_{1 \leq i \leq N}$ where N represents the number of domains. At finite temperature the Boltzmann weight associated to such a configuration can be written as

$$P_{\text{MOT}}(\ell_1, \ell_2, \dots, \ell_N, N|L) = \frac{1}{Z(L)} y^N \prod_{n=1}^N \frac{1}{\ell_n^c} \delta_{\sum_{n=1}^N \ell_n, L}, \quad (60)$$

where $\delta_{i,j}$ is the usual Kronecker delta and $c > 1$ is related to both the temperature and the long-range coupling constant. The constant y represents the fugacity which controls the number of domains N , which actually fluctuates from one configuration to another. Once again, there is a global constraint enforcing the sum rule that the domain lengths add up to the system size L . Again, this model differs slightly from the two models discussed above, namely the ZRP (55) and the renewal process (59). In the (y, c) plane, this model has a phase transition across the critical line $y_c = 1/\zeta(c)$ where $\zeta(x)$ is the Riemann zeta function. For $y > y_c$ the system is in a paramagnetic phase with a large number of domains. In contrast, for $y < y_c$, the system is ferromagnetic with one large domain of size $\propto L$. Very interesting properties emerge on the critical line $y = y_c$. In this case, for $1 < c < 2$, the largest domain size ℓ_{max} scales extensively with the system size, $\ell_{\text{max}} \propto L$ and the PDF of ℓ_{max} exhibits a scaling form [153]

$$\text{Prob.}(\ell_{\text{max}} = x, L) \approx \frac{1}{L} F_c \left(\frac{x}{L} \right), \quad (61)$$

where the scaling function $F_c(z)$ was computed exactly and was found to exhibit non-analytic behaviors at $z = 1/k$ where k is a positive integer. This scaling form (61) also indicates that the fluctuations are anomalously large in this regime. This fact was shown to be related to the so-called fluctuation-dominated phase ordering (FDPO) regime where the spin-spin correlation function develops a cusp at short distance [154]. Thus we see that, in this regime $1 < c < 2$ on the critical line $y = y_c$, the global constraint in Eq. (60) does affect the distribution of ℓ_{max} in a nontrivial way. In contrast, for $y = y_c$ but $c > 2$, one recovers the Fréchet distribution of IID random variables, indicating that the global constraint is insignificant to a large extent (it only renormalises the scale factors [153]).

4. Hierarchically and logarithmically correlated random variables

So far, we have been discussing the extreme statistics of uncorrelated, weakly correlated and strongly correlated random variables. There exists however a class of problems where the variables are *hierarchically* correlated. This is typically the case for disordered models defined on a tree. For example, one can consider the celebrated problem of a directed polymer on a tree [239]. Consider a rooted Cayley tree where each node has two off-springs. On each bond of the tree with n generations, starting from a single root at O , we assign a positive quenched random variable $\epsilon_i \geq 0$ (see Fig. 3). A configuration of $\{\epsilon_i\}$'s specifies the disordered environment. We then consider a directed polymer of n steps that goes from the root to one of the leaf sites at the n -th generation. The energy of such a directed path is given by the sum of the energies of all the bonds belonging to the path

$$E_{\text{path}} = \sum_{i \in \text{path}} \epsilon_i. \quad (62)$$

Thus there are $N = 2^n$ possible paths, each with its own energy. This model was initially studied at finite temperature $T > 0$, where it was found that it exhibits a transition to a spin-glass like (“frozen”) phase at low temperature (reminiscent of a replica symmetry breaking scenario found in mean-field spin-glasses) [239]. This problem was then revisited at $T = 0$ [12, 14] where one is interested in the path that has the *minimal* energy

$$E_{\text{min}} = \min [E_{\text{path}_1}, E_{\text{path}_2}, \dots, E_{\text{path}_N}]. \quad (63)$$

This is then a typical extreme value problem and clearly, because of the partial overlaps between the paths, the energy variables $\{E_{\text{path}_i}\}$'s are correlated. Indeed the correlations between the energies of any two paths is proportional to the number of bonds they have in common: for these reasons, the $\{E_{\text{path}_i}\}$'s are called *hierarchically correlated random variables*. It was shown in a series of work that the EVS of such random variables is closely related to traveling fronts [11–14, 17, 20, 21]. Indeed, in these cases, the cumulative distribution of the minimum (or the maximum) is generically a traveling front solution of a non-linear equation, the most well-known example being the celebrated Fisher - Kolmogorov, Petrovsky, Piskunov (F-KPP) equation. Within this connection, the number of generations

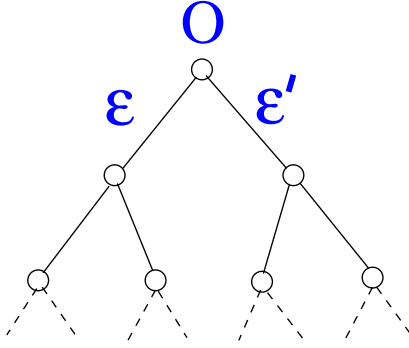


Figure 3: A Cayley tree with root node O . The root has two children, connected by edges with energies ϵ and ϵ' . Each of these children has two children of their own, and so on, with dashed lines indicating the continuation of the tree.

n plays the role of time and the average value $\langle E_{\min} \rangle$ corresponds to the position of the front. By using the tools developed to study such traveling front solutions, in particular the “velocity selection principle” that provides a criterion to select the velocity of the traveling front, one can easily compute the two leading terms (in the limit of large n) of the average value of the minimum (or the maximum).

For the directed polymer on the Cayley tree with random energies ϵ_i 's distributed according to a PDF $\rho(\epsilon)$, one can derive a recursion relation for the CDF of E_{\min} in (63), $P_n(x) = \text{Prob.}(E_{\min} \geq x)$, which reads [12]

$$P_{n+1}(x) = \left[\int \rho(\epsilon) P_n(x - \epsilon) d\epsilon \right] \left[\int \rho(\epsilon') P_n(x - \epsilon') d\epsilon' \right] = \left[\int \rho(\epsilon) P_n(x - \epsilon) d\epsilon \right]^2, \tag{64}$$

together with the initial condition $P_0(x) = \theta(-x)$. This relation follows from the following reasoning. Consider a particular realization of the disordered bond energies ϵ_i 's on a tree, as in Fig. 3. The probability $P_n(x) = \text{Prob.}(E_{\min} \geq x)$ is also the probability that all paths originating at O have energies bigger than x . Any path originating from the root O either passes through the left bond with energy ϵ or through the right bond with energy ϵ' as in Fig. 3. The left (respectively right) subtree starting with the left (respectively right) daughter of O must have energy bigger than $x - \epsilon$ (respectively $x - \epsilon'$). Hence, the probability these joint events, using the fact that the sub-trees are statistically independent, is given by the product $P_n(x - \epsilon)P_n(x - \epsilon')$, the subscript n indicates that the subtrees have n generations, as opposed to $n + 1$ for the full tree. Averaging over the bond energies, each drawn independently from the distribution $\rho(\epsilon)$ leads to the relation in Eq. (64).

To analyze the traveling front solutions of a non-linear equation of the type (64) one focuses on the left tail of $P_n(x)$, for $x \rightarrow -\infty$, where $1 - P_n(x) \ll 1$. In this regime, where Eq. (64) can be linearized, one looks for solution of the form $1 - P_n(x) \approx e^{-\lambda(x - v(\lambda)n)}$ which leads to the following dispersion spectrum [12]

$$v(\lambda) = -\frac{1}{\lambda} \ln \left[2 \int \rho(\epsilon) e^{-\lambda \epsilon} d\epsilon \right]. \tag{65}$$

For a generic distribution $\rho(\epsilon)$, the function $v(\lambda)$ admits a unique maximum at λ^* . The “velocity selection principle” states that the maximum velocity $v(\lambda^*)$ will be selected by the front [240]. One can then compute the two leading terms of $\langle E_{\min} \rangle$ in the large n limit, which generically read

$$\langle E_{\min} \rangle \approx v(\lambda^*) n + \frac{3}{2\lambda^*} \ln n. \tag{66}$$

This model of a directed polymer on a tree at zero temperature is also related to the so-called binary search tree (BST) problem in computer science. The study of BST is an important problem in computer science, with many applications related to sorting and search of data. For instance, when one stores data files in one's computer, usually one makes directories, sub-directories, sub-sub-directories, etc, which has a natural tree structure. The general idea is that, if one searches for a particular data, it is much more efficient to search if the data is stored on a tree. Typically, if the number of data elements (e.g. the number of files) stored on the tree is of size N , then a binary search takes a time of order $O(\ln N)$, which is much smaller compared to $O(N)$ for linear search. In fact, the search time is measured by the height H_N of the BST, which is the maximal depth of the nodes occupied on the tree with N occupied nodes [17]. It turns out that there is a direct mapping between the BST and the directed polymer on the Cayley tree [17].

The cumulative height distribution $P(H_N < n)$, for random data, in the BST problem is precisely related to the distribution of the minimum (ground state) energy of the directed problem discussed above. This relation in Eq. (66), in the context of the BST, translates into a result for the average height [17]

$$\langle H_N \rangle \approx \frac{1}{v(\lambda^*)} \ln N - \frac{3}{2\lambda^*v(\lambda^*)} \ln \ln N, \quad (67)$$

where $v(\lambda)$ is defined in Eq. (65) above and λ^* is the unique maximum of $v(\lambda)$. Similar traveling front solutions have also been found for other hierarchically correlated random variables, such as in a class of fragmentation models, aggregation dynamics of growing random trees, or in simple models of dynamics of efficiency (for a review see [20] and [22]). Interestingly, although the dispersion spectrum $v(\lambda)$, and consequently λ^* as well, are non-universal (i.e., they will differ from one hierarchically correlated model to another), the coefficient $3/2$ in front of the logarithmic correction in (66) turns out to be universal.

For the directed polymer on the Cayley tree, it is also possible to study the full PDF of E_{\min} in the limit of large n [14]. If the variables E_{path_i} 's were IID random variables [see e.g. Eq. (12)], the PDF of E_{\min} , properly centred and scaled, would be given (for an unbounded distribution $\rho(\epsilon)$) by a Gumbel law $F'_2(-z) = e^{z-e^z}$ (note that we are considering here the minimum, at variance with the result in Eq. (12) that concerns the maximum, which explains the '-z' in the argument). Instead of this, because the energy variables are actually hierarchically correlated, it was found that, for unbounded distribution $\rho(\epsilon)$, the limiting distribution is different from a Gumbel law. In particular, its right tail is non-universal and depends explicitly on $\rho(\epsilon)$. For instance, it was found [14] that for $\rho(\epsilon) = e^{-|\epsilon|}/2$, the limiting distribution has a simple exponential tail $\sim e^{-z}$ for $z \rightarrow +\infty$, which is quite different from the super-exponential tail of the Gumbel law.

These behaviors found for hierarchically correlated are reminiscent of the results obtained for *logarithmically* correlated random variables. For concreteness, let us indeed consider a set of N Gaussian random variables $V_1, V_2, \dots, V_i, \dots, V_N$ where the subscript i refers to a site index, which have logarithmic correlations, i.e.

$$\langle (V_i - V_j)^2 \rangle \approx 4\sigma \ln |i - j|, \quad \text{for } 1 \ll |i - j| \ll N, \quad (68)$$

where $\sigma > 0$, and denote $V_{\min} = \min\{V_1, V_2, \dots, V_N\}$. This model was first studied by Carpentier and Le Doussal [241], who found that the average value $\langle V_{\min} \rangle$ behaves indeed as described above in Eq. (63) for hierarchically correlated random variables (with the substitution $n \rightarrow \ln N$). In addition, they showed that the *left* tail of the limiting distribution of V_{\min} (properly shifted and scaled) behaves as $|z|e^z$ as $z \rightarrow -\infty$, which is indeed different from the left tail of the Gumbel law $\sim e^z$. One can further consider the simple model of a single particle in the disordered potential V_i at site i , with $i = 0, 1, \dots, N$ at thermal equilibrium at inverse temperature β . The probability p_i to find the particle at site i is thus given by the Boltzmann weight

$$p_i = \frac{1}{Z_N} e^{-\beta V_i}, \quad Z_N = \sum_{i=1}^N e^{-\beta V_i}, \quad (69)$$

where the V_i 's are Gaussian random variables with logarithmic correlations as in (68). Using Renormalization Group techniques, it was shown that this model (69) exhibits an interesting freezing phenomenon at a finite inverse temperature β_g , which is reminiscent of the transition found in Derrida's Random Energy Model (REM) [5] and its generalisations [6, 7]. Indeed, at high temperature $\beta < \beta_g$, the particle is delocalised over the whole sample while for $\beta > \beta_g$ the Boltzmann weight is concentrated on the few local minima of the disordered potential [241]. Such a freezing transition was later on confirmed by the exact solution of several models of logarithmically correlated random variables such as the equilibrium properties of single particle in random Gaussian high-dimensional landscape [70, 71, 242] or a circular variant of the REM with logarithmic correlations [71]. For these different models, the full limiting distribution of the minimum is not universal, i.e. it depends on the details of the model, but the left tail turns out to be universal, and behaves as $|z|e^z$ as $z \rightarrow -\infty$ [241]. Since then, these models have generated a lot of interest, both in physics and in mathematics, because of their relations with the extremes of the two-dimensional Gaussian Free Field (2d-GFF) [74, 243, 244]. More recently, it was suggested that the same freezing transition also governs the extreme values taken by the characteristic polynomials of random matrices and the Riemann zeta function [245, 246]. This, in turn, has generated a recent interest in mathematics [247-249], in connection with random matrices and branching processes.

5. Extreme statistics in stochastic resetting systems

We already discussed in the previous sub-section how the extreme value statistics plays an important role in binary search tree problems where the random data is stored on a binary tree. EVS has also found applications in other

intervals between resets are taken from an exponential distribution with mean $1/r$, one has $P(\tau_i) = re^{-r\tau_i}$. Averaging over τ_i , one gets the effective distribution of the minimum of the i -th block as

$$P_{\text{eff}}(m_i) = r \int_0^t d\tau_i e^{-r\tau_i} \frac{e^{-(m_i-x_0)^2/4D\tau_i}}{\sqrt{\pi D\tau_i}} \xrightarrow{t \rightarrow \infty} \alpha_0 e^{-\alpha_0(x_0-m_i)}, \quad m_i \leq x_0. \quad (70)$$

where $\alpha_0 = \sqrt{\frac{r}{D}}$ is the typical inverse length traversed by the Brownian motion between two resetting events. Therefore, the probability that the minimum of all N intervals stays above 0 is simply given by $[\int_0^{x_0} P_{\text{eff}}(m) dm]^N$. Substituting the expression for $P_{\text{eff}}(m)$ from Eq. (70), setting $N = rt$, one finds that, in terms of the rescaled length $z = \alpha_0 x_0$ the survival probability converges for large z and large t to the Gumbel form

$$Q_r(x_0, t) \approx \exp[-rt \exp(-z)]. \quad (71)$$

Therefore, this constitutes a nice application of the EVS for weakly correlated variables discussed in Section IV A. The theory of EVS can also be useful to understand the first-passage properties of other stochastic processes with resetting, going beyond the Brownian motion. This includes, for example, Lévy flights [157] and Lévy walks [162] under resetting, branching processes under restart [163, 164], active run-and-tumble particles with resetting [165], etc. We do not give further details here and refer the reader to the relevant literature cited above.

6. Extreme statistics for fluctuating interfaces in one-dimension: an example of a strongly correlated random variable

Another simple model where the extreme value statistics has been studied concerned the height fluctuations of a (1+1)-dimensional interface. As we will see below, this is an example where the relevant degrees of freedom are strongly correlated. The most well studied model of a such fluctuating interface is the so called Kardar-Parisi-Zhang (KPZ) equation that describes the time evolution of the height $H(x, t)$ of an interface growing over a linear substrate of size L via the stochastic partial differential equation [166]

$$\frac{\partial H}{\partial t} = \frac{\partial^2 H}{\partial x^2} + \lambda \left(\frac{\partial H}{\partial x} \right)^2 + \eta(x, t), \quad (72)$$

where $\eta(x, t)$ is a Gaussian white noise with zero mean and a correlator $\langle \eta(x, t)\eta(x', t') \rangle = 2\delta(x-x')\delta(t-t')$. For $\lambda = 0$, the equation becomes linear and is known as the Edwards-Wilkinson (EW) equation. For reviews on fluctuating interfaces, see e.g. [167–170]. The height is usually measured relatively to the spatially averaged height i.e.

$$h(x, t) = H(x, t) - \frac{1}{L} \int_0^L H(y, t) dy, \quad (73)$$

$$\text{with } \int_0^L h(x, t) dx = 0. \quad (74)$$

It can be shown that the joint PDF of the relative height field $P(\{h\}, t)$ reaches a steady state as $t \rightarrow \infty$ in a finite system of size L . Also the height variables are strongly correlated in the stationary state. Again in the context of the EVS, a quantity that has been studied during the last few years is the PDF of the maximum relative height in the stationary state, i.e. $P(h_m, L)$ where

$$h_m = \lim_{t \rightarrow \infty} \max_x [h(x, t), 0 \leq x \leq L]. \quad (75)$$

This is an important physical quantity that measures the extreme fluctuations of the interface heights [16, 23, 24]. We assume that initially the height profile is flat. As time evolves, the heights of the interfaces at different spatial points get more and more correlated. The correlation length typically grows as $\xi \sim t^{1/z}$ where z is the dynamical exponent ($z = 3/2$ for KPZ and $z = 2$ for EW interfaces). For $t \ll L^z$, the interface is in the ‘growing’ regime where again the height variables are weakly correlated since $\xi \sim t^{1/z} \ll L$. In contrast, for $t \gg L^z$, the system approaches a ‘stationary’ regime where the correlation length ξ approaches the system size and hence the heights become strongly correlated variables.

Following our general argument for weakly correlated variables (see Section IV A), we would then expect that in the growing regime the maximal relative height, appropriately centred and scaled, should have the Gumbel distribution. In contrast, in the stationary regime, the height variables are strongly correlated and the maximal relative height h_m should have a different distribution. This distribution was first studied numerically in [16] and then it was computed analytically in Refs. [23, 24]. This then presents one of the rare solvable cases for the EVS of strongly correlated random variables. Below, we briefly outline the derivation of this distribution.

The joint PDF of the relative heights in the stationary state can be written, taken into account the different constraints [23, 24]

$$P_{st}[\{h\}] = C(L) e^{-\frac{1}{2} \int_0^L (\partial_x h)^2 dx} \times \delta[h(0) - h(L)] \times \delta\left[\int_0^L h(x, t) dx\right], \quad (76)$$

where $C(L) = \sqrt{2\pi L^3}$ is the normalization constant and can be obtained integrating over all the heights. Note that this stationary measure of the relative heights is independent of the coefficient λ of the nonlinear term in the KPZ equation, implying that the stationary measure of the KPZ and the EW interface is the same in (1+1)-dimension (note however that this a special property of the 1 + 1-dimensional case, which breaks down for $(d + 1)$ -dimensional KPZ interfaces). The stationary measure indicates that the interface behaves locally as a Brownian motion in space [167–169]. For an interface with periodic boundary condition, one would then have a Brownian bridge in space. However, it turns out that the constraint $\int_0^L h(x, t) dx = 0$ (the zero mode being identically zero), as shown explicitly by the delta function in Eq. (76), plays an important role for the statistics of the maximal relative height [23]. It shows actually that the stationary measure of the relative heights actually corresponds to a Brownian bridge, but with a global constraint that the area under the bridge is strictly zero [23, 24]. This fact plays a crucial role for the extreme statistics of relative heights [23, 24].

We define the cumulative distribution of the maximum relative height $Q(z, L) = \text{Prob}[h_m \leq z]$. The PDF of the maximum relative height is then $P(z, L) = Q'(z, L)$. Clearly $Q(z, L)$ is also the probability that the heights at all points in $[0, L]$ are less than z and can be formally written in terms of the path integral [23, 24]

$$Q(z, L) = C(L) \int_{-\infty}^z du \int_{h(0)=u}^{h(L)=u} \mathcal{D}h(x) e^{-\frac{1}{2} \int_0^L (\partial_x h)^2 dx} \times \delta\left[\int_0^L h(x, t) dx\right] I(z, L), \quad (77)$$

where $I(z, L) = \prod_{x=0}^L \theta[z - h(x)]$ is an indicator function which is 1 if all the heights are less than z and zero otherwise. Using path integral techniques (for details see [23, 24]), it was found that the PDF of h_m takes the scaling form for all L

$$P(h_m, L) = \frac{1}{\sqrt{L}} f\left(\frac{h_m}{\sqrt{L}}\right), \quad (78)$$

where the scaling function can be computed explicitly as [23, 24]

$$f(x) = \frac{2\sqrt{6}}{x^{10/3}} \sum_{k=1}^{\infty} e^{-\frac{b_k}{x^2}} b_k^{2/3} U\left(-\frac{5}{6}, \frac{4}{3}, \frac{b_k}{x^2}\right), \quad (79)$$

where $U(a, b, y)$ is the confluent hypergeometric function and $b_k = \frac{27}{27} \alpha_k^3$, where α_k 's are the absolute values of the zeros of the Airy function: $\text{Ai}(-\alpha_k) = 0$. It is easy to obtain the small x behavior of x since only the $k = 1$ term dominates as $x \rightarrow 0$. Using $U(a, b, y) \sim y^{-a}$ for large y , we get as $x \rightarrow 0$,

$$f(x) \approx \frac{8}{81} \alpha_1^{9/2} x^{-5} \exp\left[-\frac{2\alpha_1^3}{27x^2}\right], \quad x \rightarrow 0. \quad (80)$$

The asymptotic behavior of $f(x)$ at large x can be obtained as [23, 24, 105, 280]

$$f(x) \approx 72 \sqrt{\frac{6}{\pi}} x^2 e^{-6x^2}, \quad x \rightarrow \infty. \quad (81)$$

It turns out, rather interestingly, that this same function has appeared before in several different problems in computer science and probability theory and is known in the literature as the Airy distribution function. In particular, it describes the distribution of the area under a Brownian excursion over the unit time interval (for a review on this function, its occurrence in different contexts and its generalisations see Refs. [24, 102, 171] and references therein).

The path integral technique mentioned above to compute the maximal relative height distribution of the EW/KPZ stationary interfaces have subsequently been generalised to more complex interfaces [27, 35, 76, 77, 105, 172, 173].

7. *Extreme statistics in random matrix theory*

Another beautiful solvable example of the extremal statistics of strongly correlated variables can be found in random matrices [8, 9] (see [81] for a recent review). Let us consider a $N \times N$ Gaussian random matrices with real symmetric, complex Hermitian, or quaternionic self-dual entries $X_{i,j}$ distributed via the joint Gaussian law [174, 175]

$$\Pr[\{X_{i,j}\}] \propto \exp\left[-\frac{\beta}{2} N \text{Tr}(X^2)\right], \quad (82)$$

where β is the so called Dyson index. The distribution is invariant respectively under orthogonal, unitary and symplectic transformations giving rise to the three classical ensembles: Gaussian orthogonal ensemble (GOE), Gaussian unitary ensemble (GUE) and Gaussian symplectic ensemble (GSE). The quantized values of β are respectively $\beta = 1$ (GOE), $\beta = 2$ (GUE) and $\beta = 4$ (GSE). The eigenvalues and eigenvectors turn out to be independent and their joint distribution thus factorizes. Integrating out the eigenvectors we focus here only on the statistics of N eigenvalues $\lambda_1, \lambda_2, \dots, \lambda_N$ which are all real. The joint PDF of these eigenvalues is given by the classical result [174, 175]

$$P_{\text{joint}}(\lambda_1, \dots, \lambda_N) = B_N(\beta) \exp\left[-\frac{\beta}{2} N \sum_{i=1}^N \lambda_i^2\right] \prod_{i < j} |\lambda_i - \lambda_j|^\beta, \quad (83)$$

where $B_N(\beta)$ is the normalization constant. For convenience, we rewrite the statistical weight as

$$P_{\text{joint}}(\lambda_1, \dots, \lambda_N) = B_N(\beta) \exp\left[-\beta \left(\frac{N}{2} \sum_{i=1}^N \lambda_i^2 - \frac{1}{2} \sum_{i \neq j} \ln |\lambda_i - \lambda_j|\right)\right]. \quad (84)$$

Hence, this joint law can be interpreted as a Gibbs-Boltzmann weight [176] $P_{\text{joint}}(\{\lambda_i\}) \propto \exp[-\beta E(\{\lambda_i\})]$, of an interacting gas of charged particles on a line where λ_i denotes the position of the i -th charge and β plays the role of the inverse temperature. The energy $E(\{\lambda_i\})$ has two parts: each pair of charges repel each other via a $2d$ Coulomb (logarithmic) repulsion (even though the charges are confined on the $1d$ real line) and each charge is subject to an external confining parabolic potential. Note that while $\beta = 1, 2$ and 4 correspond to the three classical rotationally invariant Gaussian ensembles described by the measure in Eq. (82), it is possible to associate a matrix model to (84) for any value of $\beta > 0$ (namely tridiagonal random matrices introduced in [177]). These ensembles defined as in Eq. (83) for generic β are sometimes called the ‘‘Gaussian β -ensembles’’. Here we focus on the largest eigenvalue $\lambda_{\max} = \max_{1 \leq i \leq N} \lambda_i$: what can be said about its fluctuations, in particular when N is large? This is a nontrivial question as the interaction term, $\propto |\lambda_i - \lambda_j|^\beta$, renders the classical results of extreme value statistics for IID random variables discussed in Section III inapplicable.

The two terms in the energy of the Coulomb gas in (84), the pairwise Coulomb repulsion and the external harmonic potential, compete with each other. While the former tends to spread the charges apart, the later tends to confine the charges near the origin. The average density of charges is given by

$$\rho_N(\lambda) = \frac{1}{N} \left\langle \sum_{i=1}^N \delta(\lambda - \lambda_i) \right\rangle, \quad (85)$$

where the angular brackets denote an average with respect to the joint PDF in Eq. (84). For such Gaussian matrices (84), it is well known [174, 175, 178] that as $N \rightarrow \infty$, the average density approaches an N -independent limiting form which has a semi-circular shape on the compact support $[-\sqrt{2}, +\sqrt{2}]$

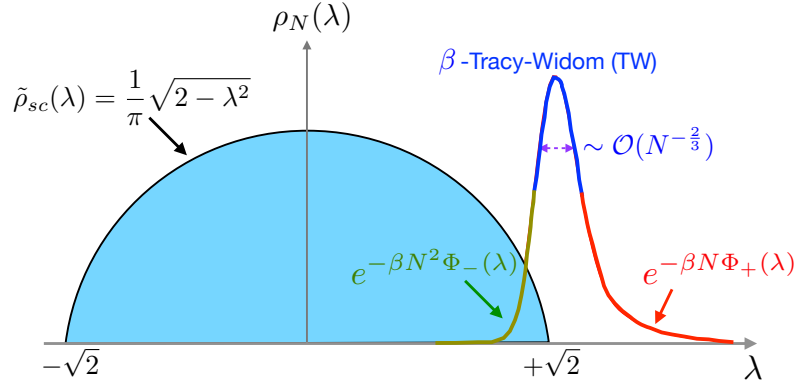
$$\lim_{N \rightarrow \infty} \rho_N(\lambda) = \tilde{\rho}_{sc}(\lambda) = \frac{1}{\pi} \sqrt{2 - \lambda^2}, \quad (86)$$

where $\tilde{\rho}_{sc}(\lambda)$ is called the Wigner semi-circular law. Hence our first observation is that the maximum eigenvalue resides near the upper edge of the Wigner semi-circle:

$$\lim_{N \rightarrow \infty} \langle \lambda_{\max} \rangle = \sqrt{2}. \quad (87)$$

However, for large but finite N , λ_{\max} will fluctuate from sample to sample and the goal is to compute its cumulative distribution

$$Q_N(w) = \text{Prob}[\lambda_{\max} < w], \quad (88)$$



$\lambda_{\max} = \sqrt{2}$ $\langle \lambda_{\max} \rangle = \sqrt{2}$
 $\mathcal{O}(N^{-2/3})$ $\mathcal{O}(1)$
typical fluctuations *atypical large fluctuations*
 $\mathcal{O}(N^{-2/3})$ $\mathcal{O}(1)$

which can be written as a ratio of two partition functions

$$Q_N(w) = \frac{Z_N(w)}{Z_N(w \rightarrow \infty)}, \tag{89}$$

$$Z_N(w) = \int_{-\infty}^w d\lambda_1 \dots \int_{-\infty}^w d\lambda_N \exp \left[-\beta \left(\frac{N}{2} \sum_{i=1}^N \lambda_i^2 - \frac{1}{2} \sum_{i \neq j} \ln |\lambda_i - \lambda_j| \right) \right]. \tag{90}$$

The partition function $Z_N(w)$ in the numerator describes a $2d$ Coulomb gas, confined on a $1d$ line and subject to a harmonic potential, as in Eq. (84), but now in the presence of an impenetrable *hard wall* at w . The study of this ratio of two partition functions reveals the existence of two distinct scales corresponding to (i) *typical* fluctuations of the top eigenvalue, where $\lambda_{\max} = \mathcal{O}(N^{-2/3})$ and (ii) *atypical* large fluctuations, where $\lambda_{\max} = \mathcal{O}(1)$.

More precisely, in the regime (i) of typical fluctuations, it can be shown that as $N \rightarrow \infty$

$$\lambda_{\max} \approx \sqrt{2} + \frac{1}{\sqrt{2}} N^{-2/3} \chi_\beta, \tag{91}$$

where χ_β is an N -independent random variable. Its cumulative distribution, $\mathcal{F}_\beta = \text{Prob}[\chi_\beta \leq x]$, is known as the β -Tracy-Widom (TW) distribution. For $\beta = 1, 2, 4$, \mathcal{F}_β can be written explicitly in terms of a special solution of a Painlevé equation [8, 9] and for $\beta = 6$ in terms of an additional Painlevé transcendent [179, 180]. For other values of β , it can be shown that \mathcal{F}_β describes the fluctuations of the ground state of a one-dimensional random Schrödinger operator, called the “stochastic Airy operator” [181, 182]. For arbitrary $\beta > 0$, it can be shown that the PDF $\mathcal{F}'_\beta(x)$ has asymmetric non-Gaussian tails [8, 9],

$$\mathcal{F}'_\beta(x) \approx \begin{cases} \exp \left[-\frac{\beta}{24} |x|^3 \right], & x \rightarrow -\infty \\ \exp \left[-\frac{2\beta}{3} x^{3/2} \right]. & x \rightarrow +\infty \end{cases} \tag{92}$$

We refer the reader to the Appendix A as well as to Refs. [183–185] and [186, 187] for more precise asymptotics of the left and right tail of the β -TW distribution respectively. Quite remarkably, the same TW distributions (in particular for $\beta = 1, 2$) have emerged in a number of a priori unrelated problems [188] such as the longest increasing subsequence of random permutations [189], directed polymers [190, 191] and growth models [192–195] in the Kardar-Parisi-Zhang (KPZ) universality class in $(1 + 1)$ dimensions as well as for the continuum $(1 + 1)$ -dimensional KPZ equation [196–199], sequence alignment problems [200], mesoscopic fluctuations in quantum dots [201–204], height fluctuations of non-intersecting Brownian motions over a fixed time interval [58, 59], height fluctuations of non-intersecting interfaces in the presence of a long-range interaction induced by a substrate [205] or more recently in the context of trapped fermions [206, 207] (see below in Section IV B 8), as well as in finance [208]. Remarkably, the TW distributions have also been observed in experiments on nematic liquid crystals [209–211] (for $\beta = 1, 2$) and in experiments involving coupled fibre lasers [212] (for $\beta = 1$).

While the β -TW distribution describes the typical fluctuations of λ_{\max} around its mean $\langle \lambda_{\max} \rangle = \sqrt{2}$ on a small scale of $\mathcal{O}(N^{-2/3})$, it does not describe atypically the large fluctuations, e.g. of order $\mathcal{O}(1)$ around $\langle \lambda_{\max} \rangle$. The probability of atypically large fluctuations, to leading order for large N , is described by two large deviations (or rate) functions $\Phi_-(w)$ (for fluctuations to the left of the mean) and $\Phi_+(w)$ (for fluctuations to the right of the mean). These different regimes for the cumulative distribution $Q_N(w)$ of λ_{\max} in Eq. (88) can be summarised, at leading order for large N , as follows

$$Q_N(w) \approx \begin{cases} \exp \left[-\beta N^2 \Phi_-(w) \right], & w < \sqrt{2} \text{ and } |w - \sqrt{2}| \sim \mathcal{O}(1) \\ \mathcal{F}_\beta \left[\sqrt{2} N^{2/3} (w - \sqrt{2}) \right], & |w - \sqrt{2}| \sim \mathcal{O}(N^{-2/3}) \\ 1 - \exp \left[-\beta N \Phi_+(w) \right], & w > \sqrt{2} \text{ and } |w - \sqrt{2}| \sim \mathcal{O}(1). \end{cases} \quad (93)$$

Equivalently, the PDF of λ_{\max} obtained from $P(\lambda_{\max} = w, N) = dQ_N(\lambda)/d\lambda$ reads, at leading order for large N (see also Fig. 5)

$$P(\lambda_{\max} = w, N) \approx \begin{cases} \exp \left[-\beta N^2 \Phi_-(w) \right], & w < \sqrt{2} \text{ and } |w - \sqrt{2}| \sim \mathcal{O}(1) \\ \sqrt{2} N^{2/3} \mathcal{F}'_\beta \left[\sqrt{2} N^{2/3} (w - \sqrt{2}) \right], & |w - \sqrt{2}| \sim \mathcal{O}(N^{-2/3}) \\ \exp \left[-\beta N \Phi_+(w) \right], & w > \sqrt{2} \text{ and } |w - \sqrt{2}| \sim \mathcal{O}(1) \end{cases} \quad (94)$$

Note that in Eqs. (93) and (94), the symbol \approx means a logarithmic equivalent. We refer to Refs. [183] and [187, 213, 214] for the study of the sub-leading corrections to the large deviations forms (93)-(94) both for the left tail and the right tail respectively. For the left tail, the rate function $\Phi_-(w)$ was first explicitly computed in Ref. [78, 79], using Coulomb gas techniques. In particular, when w approaches the critical value $\sqrt{2}$ from below behaves as

$$\Phi_-(w) \sim \frac{1}{6\sqrt{2}} (\sqrt{2} - w)^3, \quad w \xrightarrow{w < \sqrt{2}} \sqrt{2}. \quad (95)$$

For the right tail, the large deviation function $\Phi_+(w)$ was computed in Ref. [80]. A rigorous derivation (but only valid for $\beta = 1$) of $\Phi_+(w)$ can be found in [215] (see also Ref. [216] for yet another derivation of $\Phi_+(w)$ for $\beta = 1$). In particular, near $w = \sqrt{2}$ it behaves as

$$\Phi_+(w) \sim \frac{2^{7/4}}{3} (w - \sqrt{2})^{3/2}, \quad w \xrightarrow{w > \sqrt{2}} \sqrt{2}. \quad (96)$$

By inserting these asymptotic behaviors of the rate functions given by Eqs. (95) and (96) into Eq. (94), one can check that there is a smooth matching between the left and right large deviation tails and the tails of the central part described by the β -TW distribution (92) – see Ref. [81] for more details.

Interestingly, the study of the large deviations of λ_{\max} reveals the existence of a phase transition, separating the left and right tails. Indeed this corresponds to a thermodynamical phase transition for the free energy, $\propto \ln Q_N(w)$, of a Coulomb gas in the presence of a wall (89) as the position of the wall crosses the value $w_c = \sqrt{2}$. Indeed, from Eq. (93), one has

$$\lim_{N \rightarrow \infty} -\frac{1}{N^2} \ln Q_N(w) = \begin{cases} \Phi_-(w), & w < \sqrt{2}, \\ 0, & w > \sqrt{2}. \end{cases} \quad (97)$$

Since $\Phi_-(w) \propto (\sqrt{2} - w)^3$ [see Eq. (95)], the third derivative of the free energy of this Coulomb gas is discontinuous at $w_c = \sqrt{2}$: this indicates a *third order phase transition* [213]. It turns out that this transition is very similar to the so called Gross-Witten-Wadia phase transition found in the 80's in the context of $2d$ lattice quantum chromodynamics [217, 218]. As discussed in further details in [81], a similar third-order transition occurs in various physical systems, including non-intersecting Brownian motions [58, 61], conductance fluctuations in mesoscopic physics [219–221] and entanglement in a bipartite system [222, 223]. In Ref. [81], it was further argued that the universality of the TW distribution is inherited from the universality of phase transitions.

Here, we focused on the Gaussian β -ensembles (83) but extreme value questions have also been studied for a wide variety of random matrix ensembles. This includes invariant ensembles, like the Laguerre-Wishart, the Jacobi or the

Cauchy ensembles (for which all the eigenvalues are real) as well as non invariant ensembles, and in particular the so called Ginibre ensembles of RMT, for which the eigenvalues lie in the complex plane. In the latter case, the joint PDF of the complex eigenvalues can be identified with the Boltzmann weight of a two-dimensional Coulomb gas in the presence of an external quadratic confining potential, analogous to Eq. (84) but for complex eigenvalues $\lambda_i \rightarrow z_i$ where z_i 's are complex numbers. In these two-dimensional situations a natural extreme observable is the largest radius $r_{\max} = \max_{1 \leq i \leq N} |z_i|$ [224–226] (see also the discussion at the end of Section IV B 8 below). Further extensions have also been considered, either by studying various confining potentials (i.e., different from the quadratic well), which in some cases correspond to other interesting matrix models [227], or by studying Coulomb gases in higher dimensions $d > 2$ [228]. In the latter case many extreme value questions, like the distribution of the typical fluctuations of largest radius, remain open.

8. Extreme statistics of trapped fermions

More recently EVS have been studied for non-interacting fermions in a trap. Because of the Pauli principle, the positions (or momenta) of a Fermi gas are strongly correlated variables even in the absence of interactions. Remarkably, the recent developments of so called “Fermi quantum microscopes” open the possibility to probe these correlations via a direct in situ imaging of the individual fermions, with a resolution comparable to the inter-particle spacing. The theoretical understanding of these spatio-temporal correlations in noninteracting fermions is therefore a challenging problem. Many of these experiments are performed in the presence of a trapping potential, which affects the spatial correlations in a non-trivial way, as it breaks the translational invariance of the system. The physics in the bulk near the trap center (where the fermions do not feel the curvature of the confining trap) can be understood using the traditional theories of quantum many-body systems such as the local density approximation (LDA) [229]. However, away from the trap center, the fermions start feeling the curvature induced by the confining trap. As a result the average density profile of the fermions vanishes beyond a certain distance from the trap center – thus creating a sharp edge. Near this edge, the density is small (there are few fermions) and consequently, quantum and thermal fluctuations play a more dominant role than in the bulk. The importance of these fluctuations means that traditional theories such as LDA break down in this edge region [230]. Recently, there has been some progress, using techniques from RMT and determinantal processes, to study analytically this edge region (for a short review see [231]). In particular, a natural observable to probe the fluctuations at the edge is the position of the fermion which is *the farthest* from the center of the trap [206, 232], hence the connection to EVS. And since the positions of the fermions are typically strongly correlated, this is a quite hard problem.

In fact, in dimension $d = 1$ and zero temperature ($T = 0$), analytical progress can be achieved in some cases thanks to a connection between the positions of the fermions and the eigenvalues of a random matrix. Let us illustrate this on the case of N non-interacting spin-less fermions in a harmonic trap $V(x) = m\omega^2 x^2/2$. In this case, one can show that at $T = 0$ the joint PDF of the positions $P_{\text{joint}}(x_1, \dots, x_N)$, given by the modulus square of the many-body ground state wave function, reads (see e.g. [233] as well as Appendix B)

$$P_{\text{joint}}(x_1, \dots, x_N) = \frac{1}{Z_N} \exp\left(-\alpha^2 \sum_{i=1}^N x_i^2\right) \prod_{i < j} (x_i - x_j)^2, \quad (98)$$

where $\alpha = \sqrt{m\omega/\hbar}$ and Z_N is a normalization constant. By comparing this expression (98) with the joint law of the eigenvalues discussed above in Eq. (83) we see that the x_i 's behave (upto an N -dependent rescaling) like the eigenvalues of the GUE, i.e. $\beta = 2$. In particular, the position $x_{\max}(T = 0)$ of the fermion which is the farthest from the center of the trap, i.e. the rightmost fermion, has the same statistics as the largest eigenvalue λ_{\max} of a GUE matrix studied before [206]. An immediate consequence is that the distribution of $x_{\max}(T = 0)$, properly shifted and scaled, converges to the TW-distribution for the GUE, i.e. $\mathcal{F}'_2(x)$. Therefore, trapped fermions are probably the simplest physical system where the TW distribution could be observed. Interestingly, this behavior at the edge of a trapped Fermi gas is not restricted to the harmonic oscillator but actually holds (in the limit of large N) for a much wider class of smooth potentials of the form $V(x) \sim x^p$ with $p > 0$ [206, 207] (although the one-to-one correspondence with the GUE for any finite N only holds for the harmonic oscillator). Recently, it was argued that this also holds in the presence of (not too strong) interactions [234]. This edge behavior however gets modified if one considers non-smooth potentials, like a simple hard box or singular potentials. In this case, the EVS of the Fermi gas at $T = 0$ is governed by the hard-edge universality class of RMT [235, 236]. Note also that in some cases, the large deviation of $x_{\max}(T = 0)$ has also been studied [235] and they show a qualitatively similar behavior as the large deviations of λ_{\max} discussed in the previous section [see Eq. (94)]. We refer the reader to the recent review [231] for a more detailed description of these connections between one-dimensional Fermi systems at $T = 0$ and RMT.

What about the effects of finite temperature $T > 0$ on the EVS of non-interacting one-dimensional Fermi systems? At very high temperature, i.e. $T \gg E_F$ where E_F is the Fermi energy of the system, one expects that the quantum effects become negligible such that the fermions simply behave as classical independent particles. The corresponding EVS for this system is thus the one of IID random variables discussed above. Therefore, for smooth potentials like $V(x) \sim |x|^p$ the distribution of $x_{\max}(T \rightarrow \infty)$, appropriately shifted and scaled, converges to a Gumbel distribution while it converges to a Weibull distribution for a hard box potential. As T is varied, one thus expects a crossover between EVS for strongly correlated systems (like the TW distribution in the case of smooth potentials) as $T \rightarrow 0$ to the EVS of IID variables at high temperature. It turns out that the complete study of the crossover in the full temperature range from $T \rightarrow 0$ to $T \rightarrow \infty$ is highly non-trivial but it was partly studied in Ref. [206, 207] for smooth potentials. In particular, in the first case, the crossover is governed by a finite-temperature generalisation of the TW distribution which, unexpectedly, arises also in exact solution of the KPZ equation in droplet geometry at finite time [206].

The statistics of the maximal radial distance $r_{\max}(T)$ of the fermions from the trap center was also studied in dimension $d > 1$, both for smooth potentials like the harmonic well [232], and the hard box (spherical) potential [235, 236]. In both cases, although the positions of the fermions are strongly correlated at $T = 0$, it was found that, for large N , the statistics of $r_{\max}(T = 0)$ is given by the EVS of IID random variables, i.e. Gumbel for smooth potentials and Weibull for the spherical hard box. In Ref. [232] the “decorrelating” mechanism behind this was elucidated. The main idea is to decompose the many-body ground state wave function in radial and angular sectors. For each angular quantum number, one effectively obtains a one-dimensional problem for a certain number of non-interacting fermions, in an effective quantum potential characterized by the angular quantum number. In each of these angular sectors, the distribution of the farthest fermion position is non trivial. However, for spherically symmetric potentials, the different angular sectors decouple and effectively one has to look at the maximum of a collection of independent, but non-identically distributed random variables. This mechanism eventually leads to the same Gumbel or Weibull law, as for the IID case, even at zero temperature. Of course, as in the $1d$ case one also expects that at $T \rightarrow \infty$ one also recovers the EVS for IID random variables, but in this case the mechanism is quite different and the study of the description of the full crossover between these two IID regimes (as $T \rightarrow 0$ and $T \rightarrow \infty$) remains an open question. Another interesting feature of the case $d > 1$ concerns the large deviations of $r_{\max}(T)$. Indeed, it was shown in [235, 236] that, at variance with the standard scenario (94) found for instance for the β -Gaussian ensembles, there exists generically an *intermediate regime* of fluctuations between the typical and the left large deviation regime. This intermediate regime, which is actually not restricted to EVS but also concerns other observables like the full counting statistics [237], seems to be a rather generic feature of higher dimensional determinantal processes, including in particular (complex) Ginibre random matrices and two-dimensional Coulomb gas [238].

C. Other extreme value problems

1. Density of near-extremes

While the statistics of the value of the maximum is important and has interesting limiting large N behavior, as discussed extensively in this review, an equally important issue concerns the near-extreme events [28], i.e., how many events occur with their values near the extreme? In other words, the issue is whether the global maximum (or minimum) value is very far from others (*is it lonely at the top?*), or whether there are many other events whose values are close to the maximum (or minimum) value. This issue of the crowding of near-extreme events arises in many problems. For instance, in disordered systems, the zero temperature properties are completely governed by the ground-state, i.e. the state with *minimum* energy. For any finite non-zero temperature, the properties of the system are governed not just by the ground-state but the low-energy excitation states, which are just above the ground-state. Therefore, it is very important to know how many such excited states are there, above the ground-state, in an energy band $[E, E + dE]$. Such questions arise also in climate science, or in economy. For instance, for an insurance company it is very important to safeguard itself against excessively large claims. It is equally or may be more important to guard itself from an unexpectedly high number of them. Hence, it is important to know the number of insurance claims that are close to the maximal claim. In addition, in many optimization problems finding the exact optimal solution is extremely hard and the only practical solutions available are the near-optimal ones [250]. How many such solutions are there, whose costs are close to the cost of the optimal solution? In all these situations, prior knowledge about the statistics of the “crowding” of the solutions near the optimal one is very much desirable.

Consider a time series x_1, x_2, \dots, x_N of N continuous entries, which may or may not be correlated. Let $x_{\max} = \max\{x_1, x_2, \dots, x_N\}$ denote the unique maximum. A natural way to quantify the “crowding” near the maximum is

to consider the density w.r.t. the maximum [28]

$$\rho(r, N) = \frac{1}{N} \sum_{x_i \neq x_{\max}}^{N-1} \delta(r - (x_{\max} - x_i)) . \quad (99)$$

The quantity $\rho(r, N) dr$ counts the fraction of entries with values between r and $r + dr$ below the maximum, in a given realisation of the time series. Evidently, it is a random variable, which fluctuates from realisation to realisation of the time series. Note that this is different from the standard density of events, since x_{\max} itself is a random variable that fluctuates from sample to sample. An analogous quantity can be defined for a continuous time stochastic process $x(\tau)$, for $\tau \in [0, t]$

$$\rho(r, t) = \frac{1}{t} \int_0^t \delta(r - (x_{\max}(t) - x(\tau))) d\tau , \quad (100)$$

where $x_{\max}(t) = \max_{0 \leq \tau \leq t} x(\tau)$ is the global maximum of the process in $[0, t]$. The average of this quantity, either in Eq. (99) or (100) has been computed exactly (i) for a time series with IID entries, each drawn from a common parent distribution $p(x)$ [28], (ii) for a Brownian motion over a fixed time interval $[0, t]$ [98, 99] and (iii) when the x_i 's represent the N real eigenvalues of an $N \times N$ complex Hermitian matrix with Gaussian entries (the so called Gaussian Unitary Ensemble) [251, 252]. In the two latter cases, the entries of the time series are strongly correlated.

In case (i) of IID random variables, it turns out that the average of the density in Eq. (99) has been computed for all N [28]. In particular, for large N , interesting scaling behaviours emerge with universal scaling functions, depending on whether the tail of $p(x)$ for large x decays faster or slower than an exponential, with a nontrivial marginal form for the exponential tail. For the Brownian motion case (ii), not just the average but also the full distribution of $\rho(r, t)$ has been computed [98, 99]. For the GUE matrix (iii), the average has been computed for large N and its large N behaviour has found application in the computation of the average susceptibility in the random p -spin spherical model of spin-glasses [253]. We do not provide further details and the interested reader may consult the original references cited above.

2. The time at which the maximum/minimum is reached

An interesting observable associated to the statistics of extremes is the time at which the extreme occurs (see Fig. 2). For example, in a typical time series, like the price of a stock or the rainfall data, while the actual value of the extreme is important, as discussed in this article, an equally relevant question is: when does it occur? For example, in financial markets, one would naturally like to know when the price of a stock becomes maximum (that is the ideal time to sell the stock) or minimum (when one would like ideally to buy this stock). Given a stochastic process $x(\tau)$ of duration t , let t_{\max} denote the random variable such that $x(t_{\max})$ is bigger than all other values of the process in the interval $\tau \in [0, t]$. Mathematically, this is sometimes denoted as the function ‘‘argmax’’, i.e., $t_{\max} = \operatorname{argmax}[x(\tau)]$, for $\tau \in [0, t]$. Clearly, t_{\max} is a random variable, with range in $[0, t]$. A natural question then is: given t , what is the PDF of t_{\max} ? Note that the same question can be asked for a discrete time series $\{x_1, x_2, \dots, x_N\}$ of N entries. In this case, this random variable will be denoted by $n_{\max} = \operatorname{argmax}\{x_1, x_2, \dots, x_N\}$ which is clearly discrete and $1 \leq n_{\max} \leq N$.

We start with the simple example of a discrete time series $\{x_1, x_2, \dots, x_N\}$ of N IID entries, each drawn from a PDF $p(x)$. As the maximum (or the minimum) can be any one of the entries with equal probability $1/N$, it follows that the distribution of n_{\max} is just the uniform distribution

$$P(n_{\max}|N) = \frac{1}{N} \quad , \quad n_{\max} = 1, 2, \dots, N . \quad (101)$$

Thus this result is completely universal, i.e., independent of the PDF $p(x)$. While in this IID case the result is very simple and universal, one naturally wonders what is the distribution of n_{\max} when the entries of the time series are correlated, in particular when the correlations are strong, in the sense discussed before.

The simplest strongly correlated stochastic process is the continuous-time Brownian motion $x(\tau)$ [see Eq. (36)] over the time interval $\tau \in [0, t]$. In this case, the PDF of t_{\max} , denoted by $P(t_{\max}|t)$, is a continuous distribution and was computed a long time ago by P. Lévy [97]. It has a very simple expression

$$P(t_{\max}|t) = \frac{1}{\pi \sqrt{t_{\max}(t - t_{\max})}} \quad , \quad 0 \leq t_{\max} \leq t . \quad (102)$$

The corresponding cumulative distribution reads

$$\text{Prob.}(t_{\max} \leq T) = \int_0^T P(t_{\max}|t) dt_{\max} = \frac{2}{\pi} \arcsin \left(\sqrt{\frac{T}{t}} \right), \quad (103)$$

which is known as the celebrated ‘‘arcsine law’’ of Lévy. Note that the PDF (102) diverges with a square-root singularity at the two edges $t_{\max} = 0$ and $t_{\max} = t$. Since the Brownian motion starts at the origin, the event ‘‘ $t_{\max} = 0$ ’’ corresponds to trajectories that start at the origin and stay negative over the full interval $[0, t]$. In contrast, the event ‘‘ $t_{\max} = t$ ’’ corresponds to trajectories where the maximum occurs at the end of the interval $[0, t]$. Also the minimum of the curve occurs at $t_{\max} = t/2$, which is also the average value of t_{\max} . Thus instead of having a peak at its average value, the PDF has peaks at the two ends. This indicates that the typical t_{\max} is either 0 or t , while the average is $t/2$.

One can also ask the same question for a discrete-time random walk defined before in Eq. (45) where the position evolves according to $x_n = x_{n-1} + \eta_n$, starting from $x_0 = 0$ and where the jump lengths at each step are drawn independently from a symmetric and continuous distribution $f(\eta)$. Note that this includes long-range jumps such as Lévy flights, for which $f(\eta)$ has a heavy tail $f(\eta) \sim 1/|\eta|^{1+\mu}$ as $|\eta| \rightarrow \infty$ with $0 < \mu < 2$. In this case, the distribution of n_{\max} turns out to be completely universal, i.e., independent of the jump density $f(\eta)$ and is given by [254]

$$P(n_{\max}|N) = \binom{2n_{\max}}{n_{\max}} \binom{2(N - n_{\max})}{N - n_{\max}} 2^{-2N}. \quad (104)$$

This is a consequence of the celebrated Sparre Andersen theorem. For a simple derivation of this result (104), we refer the reader to Ref. [93]. In the limit of large m and n (keeping the ratio m/n fixed), one gets from Eq. (104), using Stirling’s formula

$$P(n_{\max}|N) \approx \frac{1}{\pi \sqrt{n_{\max}(N - n_{\max})}}. \quad (105)$$

Naively, this resembles the result in Eq. (102) for the Brownian motion, but this is a bit deceptive. Note indeed that this formula (105) holds even for Lévy flights, which could not have been derived from the continuous-time Brownian motion result.

The distribution of t_{\max} has also been computed, using path-integral methods, for a variety of constrained Brownian motions, such as Brownian bridge, Brownian excursion, Brownian meander, reflected Brownian motion [31, 38], Brownian motion with a drift [37], etc. These results have also been obtained using real-space renormalization group methods, which also allowed exact computation for the distribution of t_{\max} of other stochastic processes such as the continuous-time random walk (CTRW) and the Bessel process that describes the radial component of the Brownian motion in d dimensions [52]. Brownian motion, or random walks, are Markov processes. Recently, the distribution of t_{\max} has been computed exactly for some non-Markov processes. This includes the random acceleration process, i.e. $d^2x/dt^2 = \eta(t)$ where $\eta(t)$ is a Gaussian white noise [51]. Another example is the fractional Brownian motion with Hurst index $H \in [0, 1]$. The Brownian motion corresponds to $H = 1/2$ and the distribution of t_{\max} has recently been computed [107–110], using a perturbation theory around the Markov limit $H = 1/2$ developed in Ref. [255].

There have been many interesting applications of $P(t_{\max}|t)$. For example, the distribution of t_{\max} appears in a class of one-dimensional diffusion problems in a disordered potential, such as in the Sinai model. In fact, replacing t_{\max} by x and t by L , the PDF $P(t_{\max} = x|t = L)$ describes the equilibrium disordered average probability density of the position x of a particle in a disordered potential inside a box of size L [50]. Another application concerns the convex hull of Brownian motion in two-dimensions. It has been shown that, to compute the mean area of the convex hull of a two-dimensional stochastic process, the knowledge of $P(t_{\max}|t)$ of the one-dimensional component of the $2d$ motion is needed [45, 48, 128].

So far, we have been discussing the distribution of t_{\max} for a single particle problem. However, it is also interesting to ask how this distribution is affected in the presence of more than one particles, independent or interacting. For n independent Brownian motions, the distribution of t_{\max} can be computed exactly and this result has been used to compute the mean area of the convex hull of n independent Brownian motions in two-dimensions [45, 48]. An example of an interacting particle system where the distribution of t_{\max} can be computed concerns n vicious walkers in one-dimension [53]. This result has implication for $1 + 1$ -dimensional growth models belonging to the Kardar-Parisi-Zhang (KPZ) universality class [56, 62].

3. Records

We end this review by discussing briefly another topic which is intimately related to extreme statistics, namely the statistics of records which have found applications in finance, sports, climates, ecology, disordered systems, all the

way to evolutionary biology. Consider any generic time series of N entries X_1, X_2, \dots, X_N where X_i may represent the daily temperature in a given place, the price of a stock or the yearly average water level in a river. A record happens at step k if the k -th entry exceeds all previous entries. Questions related to records are obviously intimately connected to EVS. For instance the actual record value at step k is precisely the maximal value of the entries after k steps, which we have discussed in this review. In fact, as for the case of EVS, the statistics of records for IID sequences is perfectly well understood (see e. g. Ref. [256]). However, much less is known for strongly correlated time series. During the last years, important progress has been achieved in the statistics of records of random walks and Lévy flights (see e.g. [39]), which, also for records, serve as a very useful laboratory to test the effects of strong correlations and we refer the reader to the recent survey [67] for a detailed account of these results on record statistics for correlated random variables.

V. SUMMARY AND CONCLUSION

To conclude, we have made a brief overview on the subject of extreme value statistics. We have seen that for uncorrelated or weakly correlated random variables, one has a fairly good understanding of the distribution of extremum and their limiting laws: there exists essentially three limiting classes named Fréchet, Gumbel, Weibull respectively. On the other hand, there are very few exact results known for the *strongly* correlated random variables. In this review, we have discussed a few of them, but were not able to cover all of them. Most of the theoretical efforts are focussed in finding more and more exactly solvable cases which may shed some light on the issue of the universality classes of EVS for strongly correlated random variables. Identifying the universality classes (if they exist) for strongly correlated random variables is thus a very challenging and outstanding open problem.

Apart from the theoretical issue of identifying the universality classes of the extreme value distributions for strongly correlated variables, the extreme statistics of such variables also have found a large number of applications in a variety of problems arising in physics, mathematics, computer science, biology all the way to climatology or finance. In this review we have discussed very briefly some of these applications but we were not able to give an exhaustive account of these applications. For example, the largest eigenvalue of a random matrix, the limiting Tracy-Widom distributions, and also its large deviation tails, have found a wide variety of applications and have also been measured experimentally (for a brief review see [57] and the reader may also consult a couple of popular articles on the subject [257, 258]).

Going beyond the statistics of the maximum or the minimum value, there are other important and relevant questions related to extremes. For example, in this review, we have briefly touched upon some of these questions such as the density of near-extreme events, the statistics of the time at which the extreme occurs and the statistics of records. Evidently, these questions also have several applications. Another interesting topic that is of much current interest concerns the statistics of the number of maxima, minima or the saddle points of a random high-dimensional landscape. This is of interest in a variety of fields [259], including population dynamics [260, 261], models of evolutionary biology [54, 262], spin-glasses [215, 263–271], neural networks [272] as well as in landscape based string theory [273, 274] and cosmology [275]. Recently, there has been a surge of interest in these questions in the context of deep learning and artificial intelligence [276–279]. Discussing these issues is beyond the scope of this review and we may refer the reader to recent interesting reviews mentioned above.

In this short review, we have tried to give an account of the current and past research in the rapidly evolving field of extreme value statistics, in particular focusing on various physical applications of EVS. This review, by no means, provides an exhaustive list of applications of EVS in other fields, such as in biology or computer science, neither it provides details of derivations. The idea is to provide general pointers to some of the recent developments in the field in the context of statistical physics. We hope that this review will stimulate further interests and developments in this field.

ACKNOWLEDGMENTS

It is a pleasure to thank many of our collaborators and colleagues: G. Akemann, R. Allez, J. Baik, A. Bar, M. Barma, M. Battilana, G. Ben Arous, E. Ben Naim, O. Bénichou, B. Berkowitz, G. Biroli, O. Bohigas, G. Borot, J.-P. Bouchaud, D. Boyer, A. J. Bray, J. Bun, P. Calka, T. Clayes, A. Comtet, I. Corwin, F. D. Cunden, C. Dasgupta, D. S. Dean, B. Derrida, A. Dhar, D. Dhar, C. De Bacco, B. Eynard, M. R. Evans, P. J. Forrester, Y. V. Fyodorov, T. Gautier, C. Godrèche, A. Grabsch, D. Grebenkov, J. Grela, S. Gupta, A. Hartmann, H. J. Hilhorst, M. Katori, E. Katzav, M. J. Kearney, A. Krajenbrink, P. L. Krapivsky, J. Krug, A. Kundu, B. Lacroix-A-Chez-Toine, A. Lakshminarayan,

P. Leboeuf, K. Liechty, P. Le Doussal, J.-M. Luck, K. Mallick, M. Mariño, R. Marino, O. C. Martin, B. Meerson, M. Mézard, C. Monthus, F. Mori, Ph. Mounaix, D. Mukamel, C. Nadal, S. K. Nechaev, N. O’Connell, H. Orland, G. Oshanin, M. Potters, I. Perez-Castillo, A. Perret, J. Pitman, Z. Racz, J. Rambeau, K. Ramola, J. Randon-Furling, A. Rosso, S. Redner, S. Reuveni, S. Sabhapandit, A. Scardicchio, H. Schawe, C. Sire, P. Sollich, H. Spohn, C. Texier, M. Tierz, S. Tomovic, C. A. Tracy, D. Villamaina, M. Vergassola, P. Vivo, G. Wergen, S. R. Wadia, K. J. Wiese, M. Yor, O. Zeitouni, R. K. P. Zia, R. M. Ziff, A. Zoia. S.N.M. and G. S. acknowledge support from ANR grant ANR-17-CE30-0027-01 RaMaTraF.

Appendix A: Some details about the Tracy-Widom distribution

In this Appendix, we give some details about the Tracy-Widom distributions (and its generalizations), which describe the fluctuations of the largest eigenvalue in the Gaussian β -ensembles, i.e. matrix models whose eigenvalues are distributed according to Eq. (83). As stated in the text, the largest eigenvalue λ_{\max} in these ensembles behaves, in the large N limit, as

$$\lambda_{\max} = \sqrt{2} + \frac{1}{\sqrt{2}} N^{-2/3} \chi_{\beta}, \quad (\text{A1})$$

where χ_{β} is an N -independent random variable. Its cumulative distribution function (CDF), $\mathcal{F}_{\beta}(x) = \text{Prob.}[\chi_{\beta} \leq x]$, is known as the β -Tracy-Widom (TW) distribution.

The case $\beta = 2$. This case corresponds to the so-called Gaussian Unitary Ensemble (GUE) of RMT. For this special value of β , the eigenvalues form a determinantal point process and the TW distribution \mathcal{F}_2 can be written in terms of Fredholm determinant as

$$\mathcal{F}_2(s) = \text{Det}(\mathbb{I} - P_s K_{\text{Ai}} P_s), \quad (\text{A2})$$

where $K_{\text{Ai}}(x, y)$ is the so-called Airy kernel, given by

$$K_{\text{Ai}}(x, y) = \frac{\text{Ai}(x)\text{Ai}'(y) - \text{Ai}'(x)\text{Ai}(y)}{x - y} = \int_0^{\infty} \text{Ai}(x + u)\text{Ai}(y + u) du, \quad (\text{A3})$$

where Ai and Ai' denote the Airy function and its derivative respectively. We recall that a Fredholm determinant, as in Eq. (A2), is conveniently expressed by the trace expansion using $\text{Det}(\mathbb{I} - P_s K_{\text{Ai}} P_s) = \exp(-\sum_{p \geq 1} \text{Tr}(P_s K_{\text{Ai}} P_s)^p / p)$, where P_s denotes the projector on the interval $[s, +\infty)$, i.e. $[P_s K_{\text{Ai}} P_s](x, y) = \theta(x - s)K_{\text{Ai}}(x, y)\theta(y - s)$ where $\theta(z)$ is the Heaviside step function. In Ref. [8], Tracy and Widom showed that this Fredholm determinant can be written in terms of a special solution of the Painlevé II equation (the so-called Hastings-McLeod solution), denoted $q(s)$, which satisfies

$$q''(s) = 2q^3(s) + sq(s), \quad q(s) \sim \text{Ai}(s), \quad s \rightarrow \infty. \quad (\text{A4})$$

In terms of this function (A4), the TW distribution for $\beta = 2$, \mathcal{F}_2 admits a rather simple expression, namely

$$\mathcal{F}_2(s) = \exp \left[- \int_s^{\infty} (s' - s)q^2(s') ds' \right]. \quad (\text{A5})$$

We refer the reader to Ref. [213] for a derivation of this expression (A5) of the TW distribution for $\beta = 2$, without using the representation in terms of a Fredholm determinant (A2) but using instead (non-classical) orthogonal polynomials.

The case $\beta = 1, 4$. In this case, the computation of $\mathcal{F}_1(s)$ and $\mathcal{F}_4(s)$ are more complicated because the eigenvalues form a Pfaffian point process – which is a slightly more complex structure than a determinantal point process. Hence, $\mathcal{F}_1(s)$ and $\mathcal{F}_4(s)$ are then given by Fredholm Pfaffians. However, Tracy and Widom were able to reduce these Fredholm Pfaffians to Fredholm determinants [9] and from that, they could express $\mathcal{F}_1(s)$ and $\mathcal{F}_4(s)$ also in terms of the solution of the Painlevé equation (A4). Namely, they obtained [9]

$$\begin{aligned} \mathcal{F}_1(x) &= \exp \left[- \frac{1}{2} \int_x^{\infty} [(s - x)q^2(s) + q(s)] ds \right], \\ \mathcal{F}_4(2^{-\frac{2}{3}}x) &= \exp \left[- \frac{1}{2} \int_x^{\infty} (s - x)q^2(s) ds \right] \cosh \left[\frac{1}{2} \int_x^{\infty} q(s) ds \right], \end{aligned} \quad (\text{A6})$$

where $q(s)$ is given in Eq. (A4).

Other values of $\beta \neq 1, 2, 4$. For other values of β , there is no such explicit expression for $\mathcal{F}_\beta(s)$ similar to (A5) and (A6) [see however the case $\beta = 6$ Ref. [179, 180] for which $\mathcal{F}_6(s)$ can also be expressed in terms of Painlevé transcendents, albeit in a more complicated way than Eqs. (A5)-(A6)]. Nonetheless, for any generic value $\beta > 0$, the random variable χ_β in Eq. (A1) admits an interesting representation. Indeed, it can be shown that χ_β describes the fluctuations of the ground state of the following one-dimensional Schrödinger operator, called the “stochastic Airy operator” [181, 182]

$$\mathcal{H}_\beta = -\frac{d^2}{dx^2} + x + \frac{2}{\sqrt{\beta}}\eta(x), \quad (\text{A7})$$

where $\eta(x)$ is Gaussian white noise, of zero mean and with delta correlations, $\langle \eta(x)\eta(x') \rangle = \delta(x - x')$.

Precise asymptotic tails. We end up this section by indicating the precise asymptotic tail of $\mathcal{F}_\beta(s)$, beyond the leading order given in Eq. (92). The most precise asymptotic expansions, both for the right and left tail, of $\mathcal{F}_\beta(s)$ have been obtained in the physics literature by using the so-called loop-equations. For the right tail, i.e. in the limit $s \rightarrow \infty$, the asymptotic behavior of $\mathcal{F}_\beta(s)$ reads [187]

$$1 - \mathcal{F}_\beta(s) = \frac{\Gamma(\frac{\beta}{2})}{2\pi(4\beta)^{\beta/2}} s^{-\frac{3\beta}{4}} e^{-\frac{2\beta}{3}s^{3/2}} \exp \left[\sum_{m \geq 1} \frac{\beta}{2} R_m \left(\frac{2}{\beta} \right) s^{-\frac{3m}{2}} \right] \quad (\text{A8})$$

where $R_m(z)$ are polynomials with rational coefficients, of degree at most $m + 1$ and which can be computed recursively [187]. The two first leading terms in (A8) are in agreement with the rigorous result [186] $1 - \mathcal{F}_\beta(s) = s^{-\frac{3\beta}{4} + o(\ln s)^{-1/2}} e^{-\frac{2\beta}{3}s^{3/2}}$ obtained in Ref. [186] using the representation of χ_β in terms of the stochastic Airy operator (A7).

The left tail of $\mathcal{F}_\beta(s)$, for $s \rightarrow -\infty$, is also known with high precision and it reads

$$\mathcal{F}_\beta(s) = \exp \left[-\beta \frac{|s|^3}{24} + \frac{\sqrt{2}}{3}(\beta/2 - 1)|s|^{3/2} + \frac{1}{8}(\beta/2 + 2/\beta - 3) \ln |s| + c_\beta + O(|s|^{-3/2}) \right], \quad (\text{A9})$$

where c_β has a complicated, though explicit, expression [183]. This asymptotic behaviour (A9) has been proven rigorously for $\beta = 2$ in Ref. [184] and for $\beta = 1, 4$ in [185].

Appendix B: From noninteracting fermions in a harmonic trap at $T \rightarrow 0$ to random matrices

In this section, we provide the derivation of the joint PDF of the positions, given in Eq. (98), of N noninteracting fermions in a harmonic potential $V(x) = \frac{1}{2}m\omega^2 x^2$ in their ground state. The system is described by the N -body Hamiltonian

$$\mathcal{H}_N = \sum_{j=1}^N \hat{h}(\hat{x}_j, \hat{p}_j) \quad , \quad \hat{h}(\hat{x}, \hat{p}) = \frac{\hat{p}^2}{2m} + \frac{1}{2}m\omega^2 \hat{x}^2. \quad (\text{B1})$$

The single particle eigenstates $\phi_k(x)$, such that $\hat{h}\phi_k(x) = \epsilon_k \phi_k(x)$, can be obtained exactly

$$\phi_k(x) = \left[\frac{\alpha}{\sqrt{\pi} 2^{k-1} (k-1)!} \right]^{1/2} e^{-\frac{\alpha^2 x^2}{2}} H_{k-1}(\alpha x), \quad (\text{B2})$$

where $k = 1, 2, \dots$ and $H_k(z)$ is the k -th Hermite polynomial of degree k and $\alpha = \sqrt{m\omega/\hbar}$ is the characteristic length scale of the trap. The associated single-particle energy levels are given by $\epsilon_k = (k - 1/2)\hbar\omega$. The ground-state of the N -body system corresponds to filling up the N first single-particle energy levels with one fermion per level (as dictated by the Pauli exclusion principle). Correspondingly, the N -body ground-state wave-function is given by the Slater determinant

$$\Psi_0(x_1, \dots, x_N) = \frac{1}{\sqrt{N!}} \det_{1 \leq j, k \leq N} \phi_k(x_j), \quad (\text{B3})$$

with the associated energy $E_0 = \sum_{k=1}^N \epsilon_k$. The quantum probability density function (PDF) is then given by

$$P_{\text{joint}}(x_1, \dots, x_N) = |\Psi_0(x_1, \dots, x_N)|^2 = \frac{1}{N!} \left| \det_{1 \leq j, k \leq N} \phi_k(x_j) \right|^2. \tag{B4}$$

This joint PDF is normalised and encodes the quantum fluctuations of the Fermi gas. In the Slater determinant, the Gaussian factors in Eq. (B2) come out of the determinant, leaving us to compute the determinant of a matrix consisting of Hermite polynomials. The Hermite polynomials $H_0(z), H_1(z), \dots, H_{N-1}(z)$ provide a basis for polynomials of degree $N - 1$ and by manipulating the rows and columns, the determinant can be reduced to a Vandermonde determinant. Hence, we can evaluate the Slater determinant in (B4) explicitly to obtain the formula in Eq. (98).

15111116	<i>Limiting forms of the frequency distribution of the largest or smallest member of a</i>		
sample,		24,00	
15111116	<i>Statistics of Extremes</i>	24,00	
15111116	<i>Sur la distribution limite du terme maximum d'une série aléatoire,</i>		44,00
15111116	<i>Extremes and related properties of random sequences and</i>		
processes,			
15111116	<i>Random-energy model: An exactly solvable model of disordered systems,</i>	24,00	
15111116	<i>A generalization of the random energy model which includes correlations between energies,</i>		46,00
00			
15111116	<i>Solution of the generalised random energy model,</i>	19,00	
15111116	<i>Level-spacing distributions and the Airy kernel,</i>		159,00
15111116	<i>On orthogonal and symplectic matrix ensembles</i>	177,00	
15111116	<i>Universality classes for extreme-value statistics,</i>		30,00
15111116	<i>Traveling waves, front selection, and exact nontrivial exponents in a random fragmen-</i>		
tation problem,		85,00	
15111116	<i>Extremal paths on a random Cayley tree,</i>	62,00	
15111116	<i>Extremal properties of random trees,</i>		64,00
15111116	<i>Extreme-value statistics of hierarchically correlated variables deviation from Gumbel statistics</i>		
and anomalous persistence,		64,00	
15111116	<i>/f noise and extreme value statistics</i>		87,00
15111116	<i>Maximal height scaling of kinetically growing surfaces,</i>		
15111116			87,00
15111116	<i>Extreme value statistics and traveling fronts: Application to computer science,</i>		
15111116		65,00	
15111116	<i>Statistics of extremal intensities for Gaussian interfaces,</i>		
15111116		68,00	
15111116	<i>Exact solutions for the statistics of extrema of some random 1D landscapes, application to</i>		
the equilibrium and the dynamics of the toy model,		317,00	
15111116	<i>Extreme value statistics and traveling fronts: various applications,</i>		318,00
15111116	<i>Traveling front solutions to directed diffusion-limited aggregation, digital search trees, and the Lempel-Ziv</i>		
data compression algorithm,		68,00	
15111116	<i>Understanding search trees via statistical physics,</i>		64,00
15111116	<i>Exact maximal height distribution of fluctuating interfaces,</i>		92,00
15111116	<i>Airy distribution function: from the area under a Brownian excursion to the maximal height</i>		
of fluctuating interfaces,		119,00	
15111116	<i>On the area under a continuous time Brownian motion till its first-passage time,</i>		
15111116		38,00	
15111116	<i>Generalized extreme value statistics and sum of correlated variables,</i>		39,00
15111116	<i>Maximal height statistics for $1/f^\alpha$ signals,</i>		75,00
15111116	<i>Density of near-extreme events,</i>	98,00	
15111116	<i>Universal extremal statistics in a freely expanding Jepsen gas,</i>		75,00
15111116	<i>Records in a changing world,</i>		
15111116	<i>Distribution of the time at which the deviation of a Brownian motion is maximum</i>		
before its first-passage time,		66,00	

BCS	Probability distribution of the maximum of a smooth temporal signal, EE	98, 00
BCS	Universal statistical properties of poker tournaments, EE	
BKNSNR	Extreme statistics for time series: Distribution of the maximum relative to the initial value, EE	76, 00
BKNSNR	Extreme statistics for time series: Distribution of the maximum relative to the initial value, EE	76, 00
BNSNH	Condensation and extreme value statistics, EE	
ZSHB	Optimal time to sell a stock in the Black Scholes model: comment on 'Thou Shalt Buy and Hold', by A. Shiryaev, Z. Xu and XY Zhou, 00	8, 50
BSNBY	On the time to reach maximum for a variety of constrained Brownian motions, EE	41, 00
BSNBY		101, 00
0		
0000	A record-driven growth process, EE	
LNKVK	Two Bessel bridges conditioned never to collide, double Dirichlet series, and Jacobi theta function, EE	131, 00
00000	Exact Distribution of the Maximal Height of p Vicious Walkers	
0000		101, 00
0000	Maximum distributions of bridges of noncolliding Brownian paths, EE	78, 00
0000	The height and range of watermelons without wall, h International Workshop on Combinatorial Algorithms,	
0000	Convex Hull of Planar Brownian Motions: Exact Results and an Application to Ecology, EE	103, 00
00000	Driven particle in a random landscape: Disorder correlator, avalanche distribution, and extreme value statistics of records, EE	79, 00
00000	Longest excursion of stochastic processes in nonequilibrium systems, EE	
0		102, 00
000000	Random convex hulls and extreme value statistics, EE	
00000		138, 00
00000	Convex hull of a Brownian motion in confinement, EE	91, 00
0		
000000	Hitting probability for anomalous diffusion processes, EE	104, 00
0		
000000	Time at which the maximum of a random acceleration process is reached, EA	
00000	Extreme value statistics from the real space renormalization group: Brownian motion, Bessel processes and continuous time random walks, EE	
00000	Extremal statistics of curved growing interfaces in $1+1$ dimensions, EE	91, 00
0		
00000	Adaptive walks and extreme value theory, EE	107, 00
00000	Distribution of the time at which N vicious walkers reach their maximal height, EE	83, 00
0		
000000	Endpoint distribution of directed polymers in $1+1$ dimensions, 01	
0		317, 00
00000	Exact record and order statistics of random walks via first-passage ideas, 00	
00000	in "First-Passage Phenomena and Their Applications", Eds. R. Metzler, G. Oshanin, S. Redner, World Scientific (2013),	
000000	Non-intersecting Brownian walkers and Yang-Mills theory on the sphere,	
000000		844, 00
000000		857, 00
00000	Nonintersecting Brownian motions on the half-line and discrete Gaussian orthogonal polynomials, JS	
0		147, 00
00000		149, 00
00000000		150, 00
00000000		53, 00
00000000		110, 00
00000	Records in stochastic processes – Theory and applications, EE	46, 00
00000000		47, 00
00000	Applications of extreme value statistics in physics, EE	48, 00
000000	Record statistics of a strongly correlated time series: random walks and Lévy flights, EE	50, 00
0000000	Ground state energy of noninteracting fermions with a random energy spectrum, E	124, 00

0.66M	<i>How Xenopus laevis replicates DNA reliably even though its origins of replication are located and initiated stochastically,</i>	98,00	
0.66M			
0.66M	<i>On the explicit construction of Parisi landscapes in finite dimensional Euclidean spaces,</i>	86,00	
0.66M			
0.66M	<i>Statistical mechanics of a single particle in a multiscale random potential: Parisi landscapes in finite-dimensional Euclidean spaces.,</i>	41,00	
0.66M			
0.66M	<i>Freezing and extreme-value statistics in a random energy model with logarithmically correlated potential,</i>	41,00	
0.66M			
0.66M	<i>Statistical mechanics of logarithmic REM: duality, freezing and extreme value statistics of 1/f noises generated by Gaussian free fields,</i>		
0.66M	<i>Multifractality and Freezing Phenomena in Random Energy Landscapes: an Introduction,</i>	389,	
0.66M			
0.66M	<i>Universal asymptotic statistics of maximal relative height in one-dimensional solid-on-solid models,</i>	73,00	
0.66M			
0.66M	<i>Extremal statistics of curved growing interfaces in 1+ 1 dimensions,</i>		
0.66M			
0.66M	<i>Large deviations of extreme eigenvalues of random matrices,</i>	97,0	
0.66M			
0.66M	<i>Extreme value statistics of eigenvalues of Gaussian random matrices,</i>	77,	
0.66M			
0.66M	<i>Large deviations of the maximum eigenvalue for Wishart and Gaussian random matrices,</i>	102,00	
0.66M			
0.66M	<i>Top eigenvalue of a random matrix: large deviations and third order phase transition,</i>		
0.66M			
0.66M	<i>Finite-size scaling in extreme statistics,</i>	100,0	
0.66M			
0.66M	<i>Distribution of Maximal Luminosity of Galaxies in the Sloan Digital Sky Survey,</i>	759,00	
0.66M			
0.66M	<i>Renormalization-group theory for finite-size scaling in extreme statistics,</i>	81,00	
0.66M			
0.66M	<i>Renormalization flow in extreme value statistics,</i>		
0.66M	<i>Renormalization flow for extreme value statistics of random variables raised to a varying power,</i>	45,00	
0.66M			
0.66M	<i>Extreme-value distributions and renormalization group,</i>		86,
0.66M			
0.66M	<i>Large deviations of the maximum of independent and identically distributed random variables,</i>		36,
0.66M			
0.66M	<i>A first course in order statistics</i>		
0.66M	<i>Order statistics</i>		
0.66M	<i>Limit theorems for the maximum term in stationary sequences,</i>	35,00	
0.66M			
0.66M	<i>A guide to first-passage processes</i>		
0.66M	<i>Universal first-passage properties of discrete-time random walks and Lévy flights on a line: Statistics of the global maximum and records,</i>	389,00	
0.66M			
0.66M	<i>Persistence and First-Passage Properties in Non-equilibrium Systems,</i>	62,00	
0.66M			
0.66M	<i>Temporal correlations of the running maximum of a Brownian trajectory,</i>		
0.66M			
0.66M	<i>Joint distributions of partial and global maxima of a Brownian Bridge,</i>	49,00	
0.66M			
0.66M	<i>Sur certains processus stochastiques homogènes,</i>	7,00	
0.66M			
0.66M	<i>Near-extreme statistics of Brownian motion,</i>	111,00	
0.66M			
0.66M	<i>On certain functionals of the maximum of Brownian motion and their applications,</i>		
0.66M			
0.66M	<i>A stochastically quasi-optimal search algorithm for the maximum of the simple random walk,</i>	13,00	
0.66M			
0.66M	<i>The average height of planted plane trees,</i>		
0.66M			
0.66M	<i>Brownian functionals in physics and computer science,</i>	89,00	
0.66M			
0.66M	<i>Survival probability of an immobile target surrounded by mobile traps,</i>		
0.66M			
0.66M	<i>Order statistics of $1/f^\alpha$ signals</i>	84,00	

		<i>Maximum relative height of elastic interfaces in random media,</i>	
84,00			
		<i>On the maximum of a fractional Brownian motion: probability of small values,</i>	44,
		<i>Perturbative Expansion for the Maximum of Fractional Brownian Motion,</i>	94,
		<i>Extreme-Value Statistics of Fractional Brownian Motion Bridges,</i>	94,0
		<i>Pickands' constant at first order in an expansion around Brownian motion,</i>	
50,00		<i>Generalized arcsine laws for fractional Brownian motion,</i>	120,
		<i>Maximum of N independent Brownian walkers till the first exit from the</i>	
		<i>half-space</i>	43,00
		<i>Exact distributions of the number of distinct and common sites visited by N</i>	110,00
		<i>independent random walkers,</i>	
157,00		<i>Maximal distance travelled by N vicious walkers till their survival ,</i>	
		<i>Extreme statistics of non-intersecting Brownian paths,</i>	22,00
		<i>Non-crossing Brownian paths and Dyson Brownian motion under</i>	
		<i>a moving boundary,</i>	
		<i>Statistics at the tip of a branching random walk and the delay of traveling waves,</i>	
87,00			
		<i>A branching random walk seen from the tip,</i>	143,00
		<i>Maximum geographic range of a mutant allele considered as a subtype of a Brownian branching</i>	
		<i>random field,</i>	76,00
		<i>Universal order and gap statistics of critical branching Brownian motion,</i>	
112,00			
		<i>Branching Brownian motion conditioned on particle numbers,</i>	
74,00			
		<i>Spatial extent of branching Brownian motion,</i>	91,00
		<i>Large-displacement statistics of the rightmost particle of the one-dimensional</i>	
		<i>branching Brownian motion,</i>	93,00
		<i>Large deviations for the branching Brownian motion in presence of selection or coalescence ,</i>	
163,00			
		<i>Slower deviations of the branching Brownian motion and of branching random walks,</i>	
50,00			
		<i>Exact distributions of cover times for N independent random walkers in one</i>	
		<i>dimension,</i>	94,00
		<i>Cover times of random searches,</i>	11,00
		<i>Sylvester's question and the random acceleration process,</i>	
		<i>The convex hull for a random acceleration process in two dimensions,</i>	
44,00			
		<i>Area and perimeter covered by anomalous diffusion processes,</i>	15,0
		<i>Precise asymptotics for a random walker's maximum,</i>	
		<i>Survival Probability of Random Walks and Lévy Flights on a Semi-Infinite Line</i>	
50,00			
		<i>Asymptotics for the Expected Maximum of Random Walks and Lévy Flights</i>	
		<i>with a Constant Drift</i>	
		<i>An Introduction to Probability Theory and Its Applications,</i>	
		<i>A combinatorial lemma and its application to probability theory,</i>	82,00
		<i>Fonctions caractéristiques de certaines répartition définies au moyen de la notion d'ordre,</i>	
234,00			
		<i>The maximum of random walk and its application to rectangle packing,</i>	
12,00			
		<i>Mean perimeter and mean area of the convex hull over planar random</i>	
		<i>walks,</i>	
		<i>Gap statistics for random walks with gamma distributed jumps,</i>	
		<i>Gap statistics close to the quantile of a random walk,</i>	

	<i>A path transformation and its applications to fluctuation theory,</i>		59
	<i>Universal order statistics of random walks,</i>		108
	<i>Exact statistics of the gap and time interval between the first two maxima</i>		
	<i>of random walks and Lévy flights,</i>	111	
	<i>On the Gap and Time Interval between the First Two Maxima of Long Random</i>		
	<i>Walks,</i>		
	<i>On the Gap and Time Interval between the First Two Maxima of Long Continuous</i>		
	<i>Time Random Walks,</i>		
	<i>First Gap Statistics of Long Random Walks with Bounded Jumps,</i>		50
	<i>Nonequilibrium statistical mechanics of the zero-range process and related models,</i>		
		38	
	<i>Real-space Condensation in Stochastic Mass Transport Models,</i>		
	<i>Exact Methods in Low-dimensional Statistical Physics and Quantum Computing,</i>		
	<i>Extremal properties of random systems,</i>		52
	<i>The Longest Excursion of Stochastic Processes in Nonequilibrium Systems,</i>		
		102	
	<i>Statistics of the longest interval in renewal processes,</i>		
	<i>Mixed-order phase transition in a one-dimensional model,</i>		112
	<i>Mixed order transition and condensation in an exactly soluble one dimensional spin model,</i>		
	<i>Exact extreme-value statistics at mixed-order transitions,</i>		
	<i>Fluctuation-dominated phase ordering at a mixed order transition,</i>		
	<i>Diffusion with stochastic resetting,</i>		106
	<i>Diffusion with optimal resetting,</i>		44
	<i>First order transition for the optimal search time of Lévy</i>		
	<i>flights with resetting,</i>	113	
	<i>Localization transition induced by learning in random</i>		
	<i>searches,</i>	119	
	<i>Stochastic resetting in backtrack recovery by RNA polymerases,</i>		
		93	
	<i>Role of substrate unbinding in Michaelis-Menten enzymatic reactions,</i>		
		111	
	<i>Stochastic Resetting and Applications,</i>		
	<i>Optimal first-arrival times in Lévy flights with resetting,</i>		92
	<i>First passage under restart,</i>	118	
	<i>First passage under restart with branching,</i>		122
	<i>Run and tumble particle under resetting: a renewal approach,</i>		51
	<i>Dynamic scaling of growing interfaces,</i>		56
	<i>Kinetic roughening phenomena, stochastic growth, directed polymers and all that.</i>		
	<i>Aspects of multidisciplinary statistical mechanics,</i>	254	
		46	
	<i>Stochastic Processes and Random Matrices,</i>		
	<i>A KPZ Cocktail-Shaken, not stirred...,</i>		160
	<i>Brownian excursion area, Wright's constants in graph enumeration, and other Brownian areas,</i>		
		3	
	<i>The first-passage area for drifted Brownian motion and the moments of</i>		
	<i>the Airy distribution.,</i>	40	
	<i>Statistics of the first-passage time of Brownian motion conditioned by maximum value or</i>		
	<i>area,</i>	47	
	<i>Random Matrices</i>		
	<i>Log-Gases and Random Matrices</i>		
	<i>Statistical Theory of the Energy Levels of Complex Systems. I ,</i>		3
	<i>Matrix models for beta ensembles,</i>		43

81V	On the statistical distribution of the widths and spacings of nuclear resonance levels,	88P	
6	47,00		
81R	Painlevé representation of Tracy-Widom β distribution for β	68P	342,00
81R	On the Tracy-Widom β Distribution for β	68N	12,00
81R	From random matrices to stochastic operators,	68P	127,00
81R	Beta ensembles, stochastic Airy spectrum, and a diffusion,	68S	24,9
81R	Large deviations of the maximal eigenvalue of random matrices,	68S	
81R	Asymptotics of Tracy-Widom distributions and the total integral of a Painlevé II		
81R	function	68P	280,00
81R	Asymptotics of the Airy-kernel determinant,	68P	278,00
81R	The right tail exponent of the Tracy-Widom β distribution,	68P	49,00
81R	Right tail asymptotic expansion of Tracy-Widom beta laws,	68P	01,
81R	Random matrices, the Ulam problem, directed polymers & growth models, and sequence matching,	68S	
81R	Complex Systems	68P	
81R	On the distribution of the length of the longest increasing subsequence of random permu-		
81R	tations,	68S	12,00
81R	Shape fluctuations and random matrices,	68P	209,00
81R	Limiting distributions for a polynuclear growth model with external sources,	68P	100,3
81R	Universal distributions for growth processes in H dimensions and random matrices,	68P	
81R	Limit theorems for height fluctuations in a class of discrete space and time growth		
81R	models,	68P	102,00
81R	Anisotropic ballistic deposition model with links to the Ulam problem and the Tracy-		
81R	Widom distribution,	68S	69,00
81R	Fluctuations of the one-dimensional polynuclear growth model with external sources,	68N	
81R	One-dimensional Kardar-Parisi-Zhang equation: an exact solution and its universality,	68P	
81R	Free-energy distribution of the directed polymer at high temperature,	68S	
81R	Bethe ansatz derivation of the Tracy-Widom distribution for one-dimensional directed polymers,	68S	
81R	Probability distribution of the free energy of the continuum directed random polymer in		
81R	$1 + 1$ dimensions,	68P	64,00
81R	Exact asymptotic results for the Bernoulli matching model of sequence alignment,	68P	
81R	Universal gap fluctuations in the superconductor		
81R	proximity effect,	68S	86,00
81R	Density of states below the Thouless gap in a mesoscopic SNS		
81R	junction,	68S	87,00
81R	Subgap states in dirty superconductors and their effect on dephasing in Josephson qubits,	68P	
81R	Universal scaling of the order-parameter distribution in strongly disordered superconductors,	68S	87,
81R	Nonintersecting Brownian interfaces and Wishart random matrices,	68S	79,00
81R	Finite temperature free fermions and the Kardar-Parisi-Zhang		
81R	equation at finite time,	68S	114,00
81R	Non-interacting fermions at finite temperature in a d -dimensional		
81R	trap: universal correlations,	68P	94,00
81R	On the top eigenvalue of heavy-tailed random matrices,	68S	78,00
81R	Universal fluctuations of growing interfaces: evidence in turbulent liquid crystals,	68P	
81R	Growing interfaces uncover universal fluctuations behind scale invari-		
81R	ance,	68N	1,00

PKNH	<i>Evidence for geometry-dependent universal fluctuations of the Kardar-Parisi-Zhang interfaces in liquid-crystal turbulence,</i> JEP	147,80	
PKNH	<i>Measuring maximal eigenvalue distribution of Wishart random matrices with coupled lasers,</i> JEE	85,00	
PKSNM	<i>A simple derivation of the Tracy-Widom distribution of the maximal eigenvalue of a Gaussian unitary random matrix,</i> JEP		
PLF	<i>Spectral density asymptotics for Gaussian and Laguerre β-ensembles in the exponentially small region,</i> JFA	45,00	
PKGADG	<i>Aging of spherical spin glasses,</i> JEPH		120,10
PNY	<i>Complexity of random energy landscapes, glass transition, and absolute value of the spectral determinant of random matrices,</i> JRE	92,00	92,00
PKGAV	<i>Possible third-order phase transition in the large N lattice gauge theory,</i> JED		21,4
PKAV	<i>$N = \infty$ phase transition in a class of exactly soluble model lattice gauge theories,</i> JEB		93,0
PKNFB	<i>Distributions of conductance and shot noise and associated phase transitions,</i> JF	101,00	
PKSNFB	<i>Probability distributions of linear statistics in chaotic cavities and associated phase transitions,</i> JEB	81,00	
PKSNFB	<i>Phase transitions in the distribution of the Andreev conductance of superconductor-metal junctions with multiple transverse modes,</i> JEE		107,00
PKSNFB	<i>Phase transitions in the distribution of bipartite entanglement of a random pure state,</i> JEE	104,00	
PKSNM	<i>Statistical distribution of quantum entanglement for a random bipartite state,</i> JÊ	142,00	
PKR	<i>A limit theorem at the edge of a non-Hermitian random matrix ensemble,</i> JPMG		36,0
PKCF	<i>A note on the second order universality at the edge of Coulomb gases on the plane,</i> JEP	156,00	
PKGAV	<i>Large deviations of radial statistics in the two-dimensional one-component plasma,</i> JEP	164,00	
PKSNFB	<i>Extremes of 2d Coulomb gas: universal intermediate deviation regime,</i> JEPH		
PKGAV	<i>Universality of the weak pushed-to-pulled transition in systems with repulsive interactions,</i> JPH	51,00	
PKC	<i>Basic theory tools for degenerate Fermi gases in Ultra-cold Fermi Gases,</i> JPH		
PKK			
PKKAI	<i>Edge electron gas,</i> JRE	81,80	
PKSNFB	<i>Noninteracting fermions in a trap and random matrix theory,</i> JPH	52,00	
PKSNFB	<i>Statistics of the maximal distance and momentum in a trapped Fermi gas at low temperature,</i> JEP		
PKSNFB	<i>Phase transitions and edge scaling of number variance in Gaussian random matrices,</i> JRE	112,00	
PKF	<i>Free fermions at the edge of interacting systems,</i> JEP		6,00
PKSNFB	<i>Statistics of fermions in a d-dimensional box near a hard wall,</i> JEP	120,00	
PKSNFB	<i>Non-interacting fermions in hard-edge potentials,</i> JEP		
PKSNFB	<i>Intermediate deviation regime for the full eigenvalue statistics in the complex Ginibre ensemble,</i> JEPH		
PKSNFB	<i>Extremes of 2d-Coulomb gas: universal intermediate deviation regime,</i> JEPH		
PKFB	<i>Polymers on disordered trees, spin glasses, and traveling waves,</i> JEP		51,80
PKFB	<i>Front propagation into unstable states: universal algebraic convergence towards uniformly translating pulled fronts,</i> JED	146,10	
PKFB	<i>Glass transition of a particle in a random potential, front selection in nonlinear renormalization group, and entropic phenomena in Liouville and sinh-Gordon models,</i> JEE		63,00
PKCHG	<i>Classical particle in a box with random potential: exploiting rotational symmetry of replicated Hamiltonian,</i> JEB	764,80	
PKFB	<i>Tightness of the recentered maximum of the two-dimensional discrete Gaussian free field,</i> JM	65,10	

214810M	Convergence in law of the maximum of the two-dimensional discrete Gaussian free field, CPM	69,00	
214810K	Freezing transition, characteristic polynomials of random matrices, and the Riemann zeta function, SE	108,00	
214810J	Freezing transitions and extreme values: random matrix theory, and disordered landscapes, RTSA	372,00	
214810I	Maximum of the characteristic polynomial of random unitary matrices, GI	349,00	
214810H	Maxima of a randomized Riemann zeta function, and branching random walks, AD	27,00	
214810G	The maximum of the CUE field, FIN	16,00	
214810F	Statistical mechanics of combinatorial optimization problems with site disorder, SEE	72,00	
214810E	Near-extreme eigenvalues and the first gap of Hermitian random matrices, JP	156,8	
214810D	The density of eigenvalues seen from the soft edge of random matrices in the Gaussian beta-ensembles, AB	46,00	
214810C	Large time zero temperature dynamics of the spherical $p=2$ -spin glass model of finite size, JMP		
214810B	On the fluctuations of sums of random variables, H	1,00	
214810A	Perturbation theory for fractional Brownian motion in presence of absorbing boundaries, SEE	83,00	
214810Z	Records: Mathematical Theory, ACD		
214810Y	Equivalence Principle, NP	10,00	
214810X	At the far ends of a new universal law, GD		
214810W	Energy Landscapes: With Applications to Clusters, Biomolecules and Glasses GP		
214810V	Will a large complex system be stable?, N	238,00	
214810U	Stability and complexity in model ecosystems, IMP		
214810T	δ -exceedance records and random adaptive walks, JPH	49,00	
214810S	Optimal storage properties of neural network models, EA	21,00	
214810R	Spin-glass theory for pedestrians, JMP		
214810Q	Statistics of the number of minima in a random energy landscape, SEE	74,0	
214810P	Statistics of critical points of gaussian fields on large-dimensional spaces, SE		98
214810O	Phase transition in a random minima model: mean field theory and exact solution on the Bethe lattice, JMP		
214810N	Critical behavior of the number of minima of a random landscape at the glass transition point and the Tracy-Widom distribution, SE	109,00	
214810M	Random matrices and complexity of spin glasses, CPM		66,
214810L	High-dimensional random fields and random matrix theory, NR	21,00	
214810K	Complex energy landscapes in spiked-tensor and simple glassy models: Ruggedness, arrangements of local minima, and phase transitions, EX	9,00	
214810J	Topological and dynamical complexity of random neural networks, SE		110,0
214810I	The anthropic landscape of string theory in Universe or multiverse, GP		
214810H	Critical points and supersymmetric vacua I, GP		252,3
214810G	Cosmology from random multifield potentials, JP	2006.03,00	
214810F	Information, physics, and computation, GP		
214810E	Statistical-physics-based reconstruction in compressed sensing, EX	2,00	
214810D	Statistical physics of inference: Thresholds and algorithms, GP	65,00	
214810C	Comparing dynamics: Deep neural networks versus glassy systems, IMP		
214810B	Tail estimates for the Brownian excursion area and other Brownian areas, AD	12,00	
214810A	Freezing and extreme-value statistics in a random energy model with logarithmically correlated potential, JPH	41,00	
214810Z	Counting function fluctuations and extreme value threshold in multifractal patterns: the case study of an ideal $1/f$ noise JP	149,00	